Glycobiology, 2020, vol. 30, no. 5, 282–300
doi: 10.1093/glycob/cwz095
Advance Access Publication Date: 29 November 2019
Original article

OXFORD

Cancer Biology

Identification of Tn antigen O-GalNAc-expressing glycoproteins in human carcinomas using novel anti-Tn recombinant antibodies

Yasuyuki Matsumoto[2], Matthew R Kudelka[2,3], Melinda S Hanes[2], Sylvain Lehoux[2], Sucharita Dutta[2], Mark B Jones[2], Kathryn A Stackhouse[2], Gabrielle E Cervoni[2], Jamie Heimburg-Molinaro[2], David F Smith[3], Tongzhong Ju[3,4], Elliot L Chaikof[2], and Richard D Cummings[1,2,5]

[2]Department of Surgery, Beth Israel Deaconess Medical Center, Harvard Medical School, CLS 11090, 3 Blackfan Circle, Boston, MA 02115, USA, [3]Department of Biochemistry, Emory University School of Medicine, 1518 Clifton Rd, Atlanta, GA 30322, USA, [4]Office of Biotechnology Products, Center for Drug Evaluation and Research, Food and Drug Administration, Bldg 52/72, Room 2120, 10903 New Hampshire Ave, Silver Spring, MD 20993, USA and [5]Department of Surgery, Beth Israel Deaconess Medical Center, Harvard Medical School, CLS 11087, 3 Blackfan Circle, Boston, MA 02115, USA

[1]To whom correspondence should be addressed: Tel: 1.617.735.4643; e-mail: rcummin1@bidmc.harvard.edu, rcummin1@bidmc.harvard.edu

Received 8 August 2019; Revised 8 October 2019; Editorial Decision 2 November 2019; Accepted 2 November 2019

Abstract

The Tn antigen is a neoantigen abnormally expressed in many human carcinomas and expression correlates with metastasis and poor survival. To explore its biomarker potential, new antibodies are needed that specifically recognize this antigen in tumors. Here we generated two recombinant antibodies to the Tn antigen, Remab6 as a chimeric human IgG1 antibody and ReBaGs6 as a murine IgM antibody and characterized their specificities using multiple biochemical and biological approaches. Both Remab6 and ReBaGs6 recognize clustered Tn structures, but most importantly do not recognize glycoforms of human IgA1 that contain potential cross-reactive Tn antigen structures. In flow cytometry and immunofluorescence analyses, Remab6 recognizes human cancer cell lines expressing the Tn antigen, but not their Tn-negative counterparts. In immunohistochemistry (IHC), Remab6 stains many human cancers in tissue array format but rarely stains normal tissues and then mostly intracellularly. We used these antibodies to identify several unique Tn-containing glycoproteins in Tn-positive Colo205 cells, indicating their utility for glycoproteomics in future biomarker studies. Thus, recombinant Remab6 and ReBaGs6 are useful for biochemical characterization of cancer cells and IHC of tumors and represent promising tools for Tn biomarker discovery independently of recognition of IgA1.

Key words: anti-Tn antibody, diagnostic biomarker, human chimeric antibody, TACA, Tn-containing glycoproteins

Statement of Significance: Recombinant engineered versions of anti-Tn antigen antibodies specifically recognize Tn on glycoproteins from tumor cells and tumor tissues but not on normal tissue or IgA1, creating potential for biomarker and therapeutic avenues.

Introduction

Altered glycosylation is a hallmark of cancer, and aberrant glycan structures, or tumor-associated carbohydrate antigens (TACAs), are biomarkers of tumor progression (Hakomori 2001; Fuster and Esko 2005). A highly relevant TACA is the Tn antigen (GalNAcα1-Ser/Thr), which is a truncated form of O-GalNAc mucin-type O-glycans. The expression of the Tn antigen and sialylTn (STn) in tumors represent potential markers associated with poor prognosis and tumor metastasis (Ju et al. 2013; Ju et al. 2014; Kudelka et al. 2015; Stowell et al. 2015; Chia et al. 2016). The Tn antigen is a biosynthetic precursor to all extended O-GalNAc glycans in human cell glycoproteins and is generated by 1 of 20 polypeptide *N*-acetylgalactosaminyltransferases (ppGalNAc-Ts) (Bennett et al. 2012). In normal tissues, the Tn antigen is not expressed on mature surface membrane glycoproteins, as it is efficiently modified by a single enzyme, the T-synthase (encoded by *C1GALT1*), which in the Golgi apparatus transfers a galactose residue onto Tn to form the core 1 O-glycan structure (Galβ1-3GalNAcα1-Ser/Thr) that can be further modified with other sugars (Ju and Cummings 2002a, b). The biosynthesis of active T-synthase requires a specific molecular chaperone, Cosmc (encoded by the X-linked *C1GALT1C1*), which functions in the endoplasmic reticulum to assist folding and activity of the T-synthase. Importantly, acquired mutations or alterations in Cosmc expression have been associated with many human cancers, including pancreatic cancer, where the Tn antigen is typically highly expressed (Ju et al. 2008; Radhakrishnan et al. 2014; Jiang et al. 2018).

In many studies, the expression of the Tn antigen is examined using plant lectins, but some use monoclonal antibodies, whose specificities may not be limited to the Tn antigen (Yuan 1989; Itzkowitz et al. 1992; Schumacher et al. 1994; Mitchell and Schumacher 1999; Kudelka et al. 2015). Another complication is that many anti-Tn reagents recognize terminal α-linked GalNAc residues and could possibly bind to that residue in blood group A (BGA), Forssman-related antigens and IgA1. The latter is a confounding factor to the potential use of the Tn antigen as a tumor biomarker, as circulating glycoforms of human IgA1 contain the Tn antigen in the hinge region (Lehoux et al. 2014). Thus, any antibody that binds the Tn antigen and also Tn-positive IgA1 glycoforms would have limited usefulness. Furthermore, while several potentially Tn-positive glycoproteins, such as mucins CA15-3 (MUC1) and CA125 (MUC16), have been developed for clinical use to follow cancer progression (Aithal et al. 2018; Taylor-Papadimitriou et al. 2018), the expression and identification of the mucin protein epitopes are not specific enough for use in cancer diagnosis. As the Tn antigen might be present in several tumor-specific Tn-positive glycoproteins released into plasma, we sought to generate specific antibodies with restricted specificity to the Tn antigen on glycoproteins and lacking recognition of IgA1.

To this end, we generated a novel, recombinant human chimeric IgG1 anti-Tn antibody, named Remab6, derived in part from an original murine anti-Tn ascites (Ca3638, BaGs6) (Springer et al. 1990). We also generated a recombinant murine IgM of this antibody, ReBaGs6, which allows direct comparison of the experimental results obtained with the ascites to those obtained with the recombinant ReBaGs6. Our studies show that these antibodies have high affinity and are remarkably specific for the Tn antigen with no recognition of human IgA1, and are useful in immunohistochemistry (IHC) with a variety of human cancers. Thus, these antibodies represent new useful reagents to detect Tn-positive glycoproteins as a biomarker for human carcinomas and may also be a novel therapeutic agent for targeted cancer treatment.

Results

Affinity purification of the Tn-reactive IgM from BaGs6 ascites

BaGs6 is a murine IgM arising from immunization with Tn-positive cells and available only as a mouse ascites fluid (Springer et al. 1990). Our previous microarray studies demonstrated that among all types of potential anti-Tn monoclonal antibodies we screened, BaGs6 was the most specific and recognized di- and tri-Tn clustered structures on mucin glycopeptides (Borgert et al. 2012). Flow cytometry data also demonstrated that BaGs6 specifically interacts with Tn-positive LS174T and MDA-MB-231 cells, similarly to the lectin *Vicia villosa* agglutinin (VVA), which indiscriminately recognizes terminal α-linked GalNAc on most types of glycoconjugates (Tollefsen and Kornfeld 1983) (Supplementary Fig. S1A). However, unlike VVA, binding of BaGs6 was incompletely inhibited by GalNAc, but was efficiently inhibited by Asialo-BSM, a mucin that contains a high density of Tn sites (Tsuji 1986) (Supplementary Fig. S1B). Although VVA was also inhibited by Asialo-BSM, inhibition was only observed at the highest concentration tested. Neither BaGs6 nor VVA were inhibited by lactose. A western blot showed that both BaGs6 and VVA bind to multiple species with different molecular masses in Tn-positive cells (Supplementary Fig. S1C). This demonstrates that BaGs6 and VVA differ in their recognition of glycoproteins.

To isolate BaGs6 from the ascites fluid, we conjugated Asialo-BSM at highest densities to UltraLink beads to generate a high avidity Tn-rich resin (Figure 1A). The ability of the affinity resin to bind BaGs6 was characterized by fluorescence microscopy, which demonstrated that the ascites-derived BaGs6 strongly interacted with Asialo-BSM resin, little with BSM resin, and did not interact with the unconjugated control beads (as detected by anti-IgM secondary antibody alone) (Figure 1B). BaGs6 was successfully affinity-purified from the ascitic fluid and appeared homogeneous by Coomassie staining (Figure 1C). The affinity-purified BaGs6 was sequenced de novo using LC-MS/MS to generate a predicted amino acid sequence. Because of the uncertainty regarding the presence of leucine/isoleucine and some other residues, we engineered a recombinant antibody with an appropriately chosen amino acid sequence; the sequence for the complementarity determining regions (CDRs) within its variable regions are shown in Figure 1D. The CDRs of BaGs6 were compared to those in three other known anti-Tn antibodies, 83D4 (Pancino et al. 1990), MLS128 (Numata et al. 1990) and 5E5 (Sorensen et al. 2006). CDR3 is generally considered to be an essential region to determine the specificity of an antibody (Xu 2000). Interestingly, CDR3 in heavy chain and CDR1–3 in light chain of BaGs6 exhibited significant diversity from the other available sequenced anti-Tn antibodies (Figure 1D), suggesting that the binding specificity of BaGs6 will be somewhat different from the other antibodies.

Generation of Remab6, a chimeric anti-Tn IgG1 and ReBaGs6, a mouse anti-Tn IgM

Using the sequence information, we generated a recombinant antibody designated Remab6, which is a chimeric IgG1 and contains partial sequences of the mouse variable region from BaGs6 and the

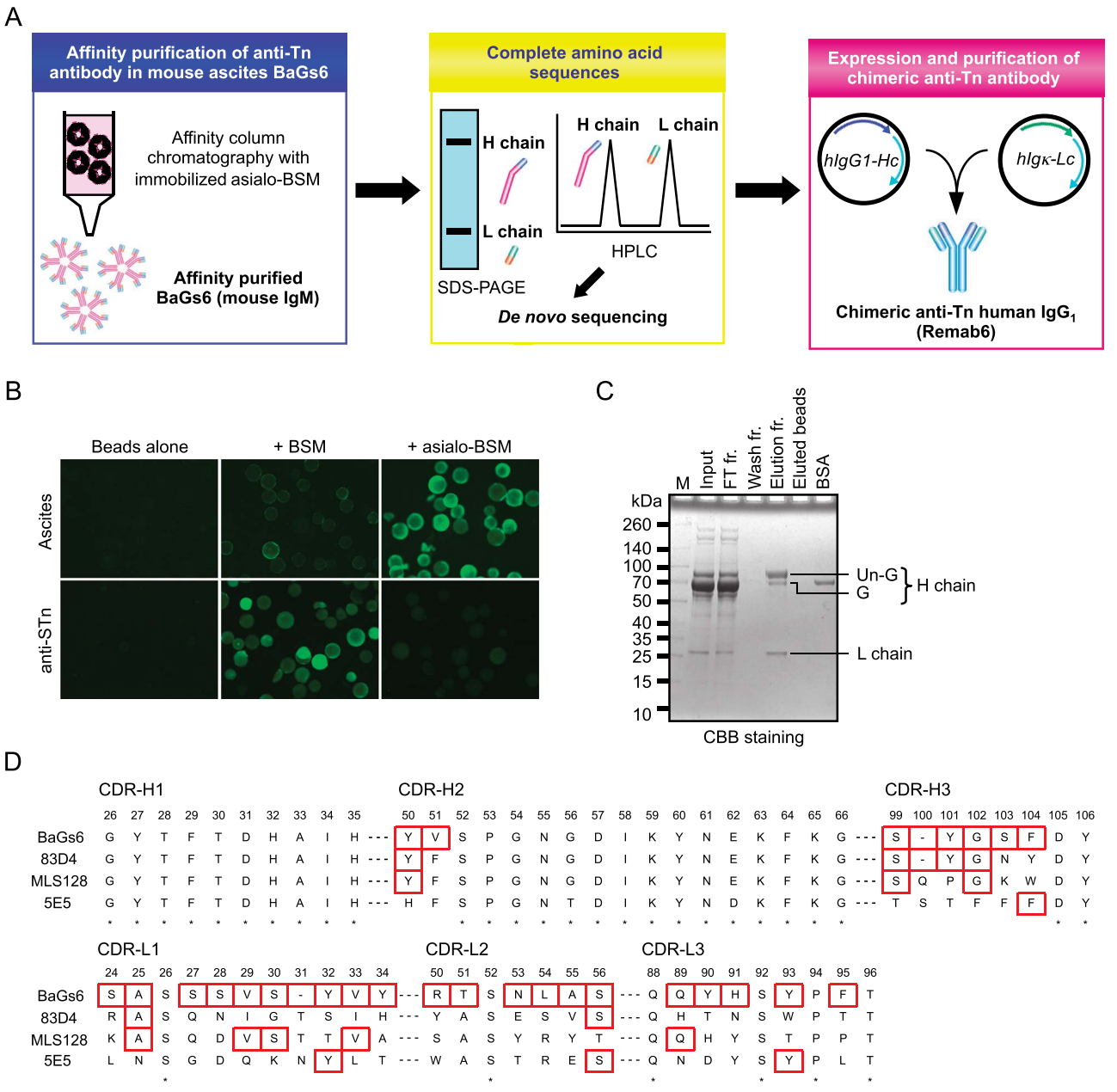

Fig. 1. Overview of the experimental workflow and identification of complete amino acid sequence of BaGs6. (**A**) Mouse ascites BaGs6 (IgM) antibody, reactive to Tn antigen and used in a number of publications as a cancer biomarker, was purified using affinity chromatography with immobilized Asialo-BSM which carries a high density of Tn antigen. From complete amino acid sequences, the recombinant Tn antigen-specific human IgG1, named Remab6, was purified and characterized. (**B**) Asialo-BSM beads were prepared by neuraminidase treatment of BSM beads. High-density Asialo-BSM beads were stained with ascites or anti-STn antibody confirmed by microscopy analysis. (**C**) BaGs6-containing mouse ascites were affinity-purified with Asialo-BSM beads. (**D**) Complete amino acid sequences were determined by proteomic de novo sequencing and CDRs of H chain (top) and L chain (bottom) were compared between three established anti-Tn antibodies (83D4, MLS128 and 5E5). ∗ indicates identical residues in all four antibodies. Red boxes indicate different residues between BaGs6 and one or more of the antibodies.

human constant region of IgG1. We chose to first generate IgG1, due to its high utility in a number of biochemical assays, as well as ease of analysis and coupling to Protein A/G-Sepharose. It is also specifically recognized by common anti-human Ig reagents, making it useful in murine studies where no interference with murine Ig would occur. Furthermore, we also generated recombinant BaGs6 (ReBaGs6), a murine IgM (mIgM), which includes the mouse variable region and the mouse constant region of IgM. Both Remab6 and ReBaGs6 were expressed in human HEK293 cells and purified (Figure 2A).

Microarray studies of Remab6 and ReBaGs6 show specificity to a subset of Tn glycopeptides

We compared the specificity of Remab6 and ReBaGs6 on a Tn glycopeptide microarray (Table I), which contains many peptides with one or more Tn antigens, including peptides modeled after the hinge region of human IgA1. These antibodies showed similar recognition patterns to that of the original mouse ascites (Figure 2B). Both Remab6 and ReBaGs6 recognized di- and tri-Tn clustered

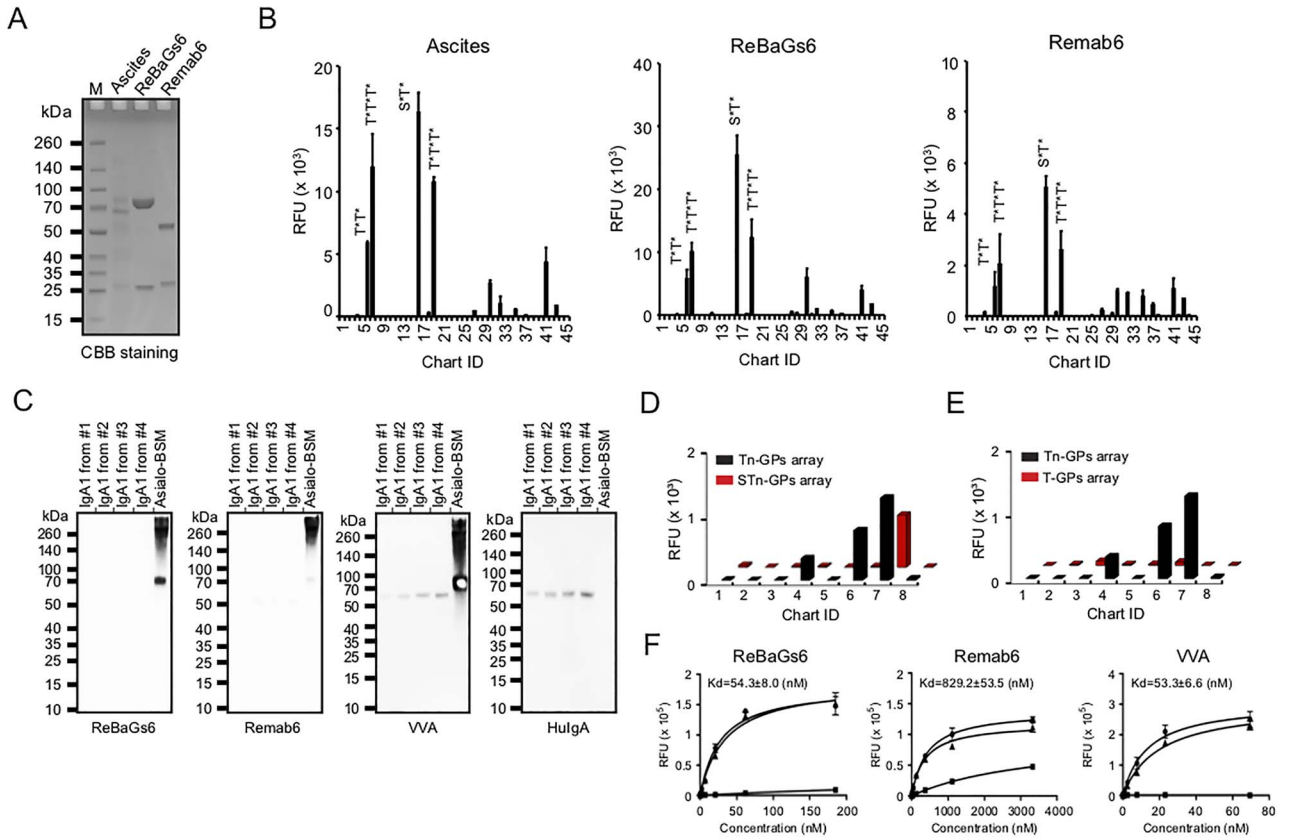

Fig. 2. Remab6 is specific for Tn glycopeptides, but not Tn on IgA1, STn, T glycopeptides, BGA or glycans expressing terminal GalNAc. (**A**) Remab6 and ReBaGs6 were recombinantly expressed in the HEK293 freestyle expression system. The purified Remab6 and ReBaGs6 were separated by SDS-PAGE and stained by CBB solution. (**B**) Tn glycopeptide (GP) array was probed with ReBaGs6 (middle) and Remab6 (right) to compare to the specificity of the original mouse ascites (left). Chart ID corresponds to Table I. (**C**) Western blots with IgA1 purified from four individual healthy donor serum (control: Asialo-BSM) were probed with ReBaGs6, Remab6, lectin VVA and goat anti-human IgA antibody. (**D–E**) Enzymatically remodeled Tn glycopeptide array slides to create STn (**D**) and T (**E**) antigen glycopeptides (ID1–8). STn and T glycopeptide arrays were probed with Remab6. Error bars represent ±1 SD of four replicates. (**F**) Affinity constants were measured for ReBaGs6 (left), Remab6 (middle) and VVA (right) by Asialo-BSM-coated plate. Circle (nontreated), square (pretreated with 100 mM GalNAc) and triangle (pretreated with 100 mM GlcNAc) were plotted. Error bars represent SD of two replicates. RFU = relative fluorescence units.

structures on mucin-derived glycopeptides, but only weakly interacted with synthetic glycopeptides containing the Tn antigen on IgA1 (Figure 2B). As circulating IgA1 has two distinct glycoforms as previously described (*Helix pomatia* agglutinin (HPA)+/Peanut agglutinin (PNA)−, which are Tn/STn-positive; HPA−/PNA+, which represent extended O-glycans) (Lehoux et al. 2014), we tested whether both Remab6 and ReBaGs6 bound to Tn antigen on IgA1 from Dakiki B cells in which the *Cosmc* gene was deleted and thus express Tn antigen on the cell surface as well as on their secreted IgA1. IgA1 in total cell extracts was examined for its binding to Remab6, ReBaGs6 and VVA. Consistent with Tn glycopeptides array results, both Remab6 and ReBaGs6 bound only to Tn-expressing glycoproteins in *Cosmc* KO Dakiki cell extracts, but not the Tn antigen on IgA1, whereas VVA bound well to IgA1 (Supplementary Fig. S2). We also tested the binding of both Remab6 and ReBaGs6 towards native human IgA1 from four donors by western blot and observed no binding (Figure 2C). These results demonstrate that both Remab6 and ReBaGs6 bind glycoproteins expressing the Tn antigen, but are unable to bind to IgA1 glycoforms expressing the Tn antigen.

We also defined interactions of Remab6 with Tn derivatives, e.g. STn (Neu5Acα2-6GalNAcα1-Ser/Thr) and T (Galβ1-3GalNAcα1-Ser/Thr) antigens, by enzymatically synthesizing them directly on the Tn glycopeptide array (Supplementary Fig. S3). Partial sialylation of Tn antigen with recombinant ST6GalNAc-I to generate STn significantly decreased binding of Remab6, with the signal remaining above background only for the MUC2 glycopeptide containing three consecutive Tn sites (ID7) (Figure 2D). In the microarray platform, we suspected that perhaps the three adjacent Tn sites could not be efficiently sialylated, compared to the same peptide sequence with two adjacent Tn sites (ID6), and therefore the binding signal observed after sialylation was due to the incomplete Tn sialylation reaction. To test this hypothesis, we characterized the reaction product after sialylation in solution by MALDI-TOF MS analysis and found that the triple-Tn-MUC2 (ID7) substrate was much less efficiently sialylated than the double-Tn-MUC2 (ID6) substrate (Supplementary Fig. S3A). In fact, a strong signal from the nonsialylated peptide was present after the reaction. We also enzymatically synthesized a T glycopeptide array by incubating the Tn glycopeptide array slides with recombinant T-synthase, thus modifying the Tn antigen by addition of β1,3-linked galactose. This modification inhibited Remab6 binding (Figure 2E, Supplementary Fig. S3B). Furthermore, both Remab6 binding and ReBaGs6 binding to Asialo-BSM were inhibited by addition of soluble GalNAc, but not GlcNAc.

More importantly, ReBaGs6 exhibited a relatively strong binding to glycoproteins with the Tn antigen ($K_d = 5.43 \times 10^{-8}$ M), while

Table I. Structures printed on the Tn glycopeptide array

Chart ID	Detail	Sequence
1	A-MUC2	Ac-PT∗TTPLK-NH2
2	B-MUC2	Ac-PTT∗TPLK-NH2
3	C-MUC2	Ac-PTTT∗PLK-NH2
4	D-MUC2	Ac-PT∗T∗TPLK-NH2
5	E-MUC2	Ac-PT∗TT∗PLK-NH2
6	F-MUC2	Ac-PTT∗T∗PLK-NH2
7	G-MUC2	Ac-PT∗T∗T∗PLK-NH2
8	R-MUC2	Ac-PTTTPLK-NH2
9	a-Dystroglycan	Ac-PPTTTTKKP-NH2
10	MUC5AC	H2N-GTTPSPVPT∗TSTTSAP-OH
11	EA2	Ac-PTTDSTT∗PAPTTK-NH2
12	EA2-R	Ac-PTTDSTTPAPTTK-NH2
13	a-Dystroglycan	Ac-PPT∗T∗T∗T∗KKP-HN2
14	MUC1–1	H2N-TSAPDT∗RDAP-NH2
15	MUC1–1R	H2N-TSAPDTRDAP-NH2
16	MUC1–2	H2N-APGS∗T∗APP-NH2
17	MUC1–2R	H2N-APGSTAPP-NH2
18	PADRE Tn3b	H2N-GaKcVAAWTLKAAaT∗T∗T∗G-CONH2
19	Tn3 linker	Ac-T∗T∗T∗-NH(CH2)3NH2
20	Tn linker	Ac-T∗-NH(CH2)3NH2
21	Peptide-4	H2N-KTTT-CONH2
22	Peptide-5	H2N-KTTTG-CONH2
23	Ser-GalNAc1	H2N-Ser(a-D-GalNAc)-NH2
24	Ser-GalNAc2	H2N-Ser(a-D-GalNAc)-OH
25	Thr-GalNAc1	H2N-Thr(a-D-GalNAc)-NH2
26	Thr-GalNAc2	H2N-Thr(a-D-GalNAc)-OH
27	IgA-Pep01	H2N-KPVPST∗PPT∗PS∗C-OH
28	IgA-Pep02	H2N-KPVPSTPPTPSC-OH
29	IgA-Pep03	H2N-KPVPS∗TPPTPSC-OH
30	IgA-Pep04	H2N-KPST∗PPT∗PS∗PS∗C-OH
31	IgA-Pep05	H2N-KPSTPPTPSPSC-OH
32	IgA-Pep06	H2N-KT∗PPT∗PS∗PS∗TPC-OH
33	IgA-Pep07	H2N-KTPPTPSPSTPC-OH
34	IgA-Pep08	H2N-KTPPTPSPST∗PC-OH
35	IgA-Pep09	H2N-KPT∗PS∗PS∗TPPT∗C-OH
36	IgA-Pep10	H2N-KPSPSTPPTPSC-OH
37	IgA-Pep11	H2N-KPS∗PS∗TPPT∗PSC-OH
38	IgA-Pep12	H2N-KPSTPPTPSPSC-OH
39	IgA-Pep13	H2N-KPS∗TPPT∗PSPSC-OH
40	IgA-Pep14	H2N-KPSTPPTPSPSC-OH
41	IgA-Pep15	H2N-KPST∗PPTPS∗PS∗C-OH
42	IgA-Pep16	H2N-KPSTPPTPS∗PSC-OH
43	IgA-Pep17	H2N-KPSTPPTPSPS∗C-OH
44	IgA-Pep18	H2N-KPST∗PPTPSPSC-OH
45	Phosphate Buffer	

* GalNAc on serine or threonine. For PADRE Tn3b; a=D-alanin, c=Cyclohexylalanine.

Remab6 as a chimeric human IgG1 showed a slightly lower binding affinity ($K_d = 8.29 \times 10^{-7}$ M). The binding constant of ReBaGs6 is close to that of VVA (Figure 2F). Finally, the CFG mammalian glycan microarray results show that Remab6 does not bind to BGA, Tn-related glycans or other glycans expressing terminal α-GalNAc (Supplementary Fig. S4). These results demonstrate that Remab6 is highly specific to the Tn antigen, especially in the clustered Tn-glycopeptide form, but does not detectably interact with STn antigen, T antigen or Tn antigen on human IgA1.

Remab6 robustness in flow cytometry and immunofluorescence applications

Like BaGs6, Remab6 stained a variety of Tn-positive Simple Cell lines by flow cytometry, but not their Tn-negative counterparts for LSC/LSB, LS174T, Colo205, MDA-MB-231, MKN-45 and Jurkat cell lines (Figure 3A). Confocal microscopy analysis with Remab6 showed similar selectivity to Tn-positive cells in the MDA-MB-231 cell line. Staining was observed on the cell surface and intracellular compartments, which was less co-localized in *cis*-medial Golgi

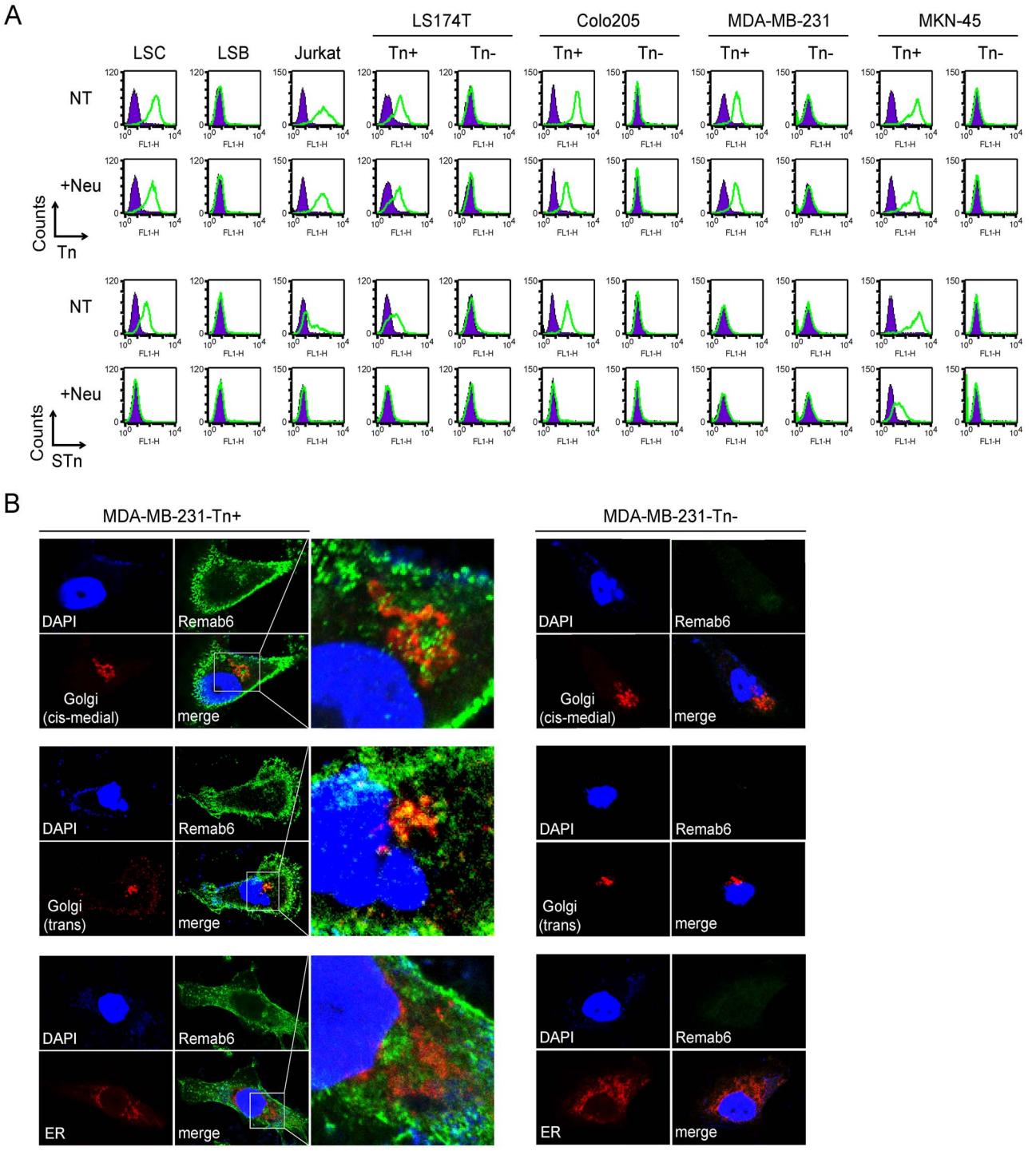

Fig. 3. Binding profiles and distribution of Tn-carrying molecules within cells. (**A**) Flow cytometry profiles using Remab6 (top) and anti-STn antibody (bottom) without (NT) or with treatment with neuraminidase (+Neu) on colorectal, breast, gastric carcinoma and leukemic cell lines. (**B**) Immunofluorescence studies showing localization of Tn+ staining with respect to nuclear (DAPI), *cis*-medial Golgi (Giantin; top), trans Golgi (TGN46; middle) and ER (Calnexin; bottom) of Tn-positive (left) and Tn-negative (right) MDA-MB-231 cell lines. Images were collected by confocal microscopy (Zeiss).

than trans Golgi apparatus but not co-localized in ER (Figure 3B and Supplementary Fig. S5). These data demonstrate that Remab6 is a specific reagent for a variety of biochemical assays and can be used to distinguish intracellular vs. extracellular Tn antigen presentation.

Immunohistochemical staining in IEC-Cosmc KO mice and human cancer cell block sections and human cancer tissue array

To further define the specificity of Remab6 using mammalian tissues, and whether Remab6 is specific to tissues expressing the

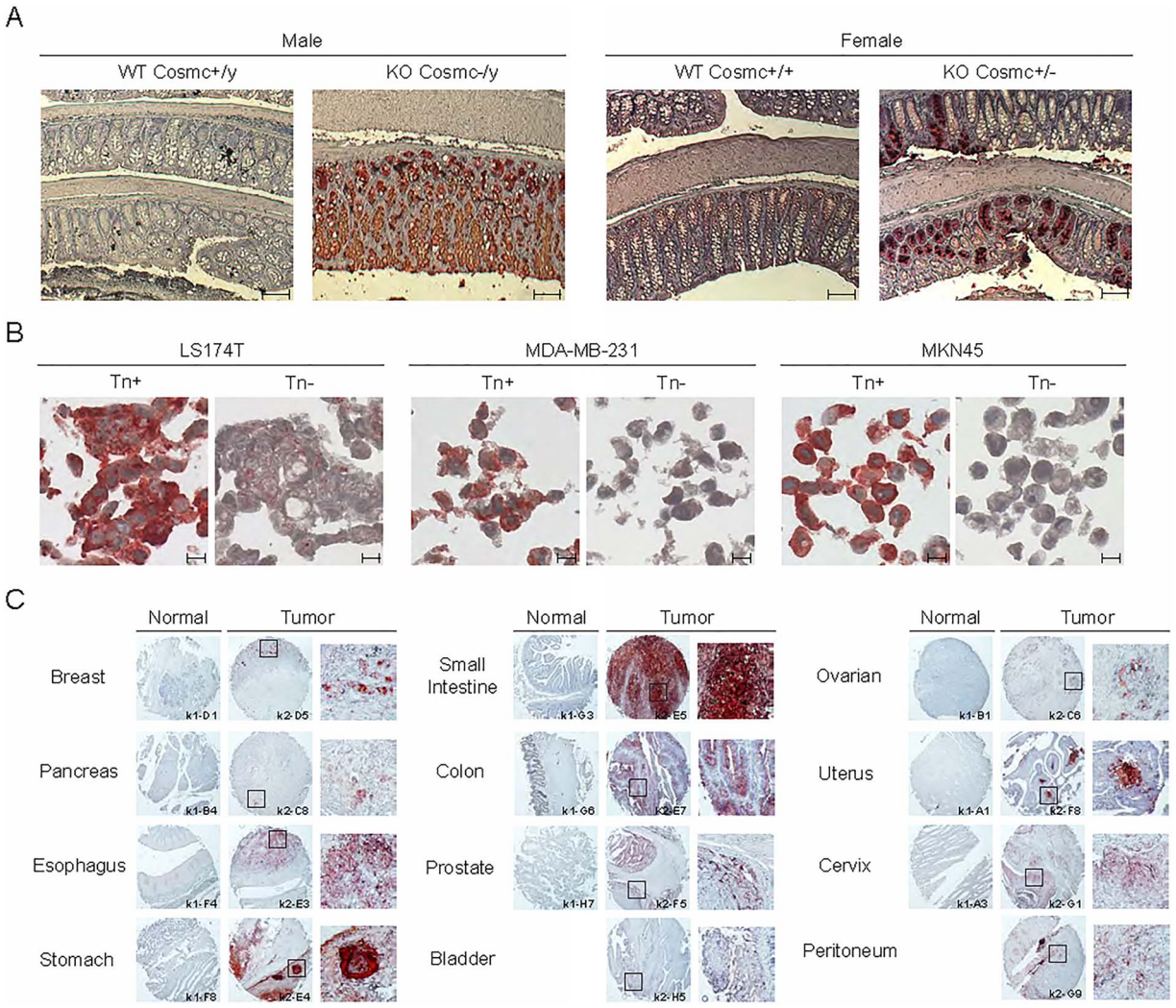

Fig. 4. Immunohistochemical staining in IEC-*Cosmc* KO mice and human cancer cell block sections, and human cancer tissue array. (**A**) IHC staining with Remab6 using small intestine-colon-rectum sections in villi-specific *Cosmc* KO mice (male; KO *Cosmc*$^{-/y}$, female; KO *Cosmc*$^{+/-}$) compared to WT. Scale bar represents 100 µm. (**B**) Cell block section staining with Remab6 of Tn-positive or Tn-negative populations of human carcinoma cell lines (LS174T, MDA-MB-231 and MKN-45). Scale bar represents 10 µm. (**C**) Human cancer tissue array (FDA808k-1/2, US Biomax Inc.), including normal and tumor tissues as indicated, with Remab6-Fab-HRP reagent. Squares represent Tn-positive staining sites with high magnification. Brownish-red indicates Tn staining with antibody, and blue indicates nuclear staining.

Tn antigen on glycoproteins, we exploited our prior development of the IEC-*Cosmc* KO mice, which abundantly express the Tn and STn truncated O-glycans in the colorectum and small intestine in male KO and exhibit ~50% expression in female mosaics (Kudelka et al. 2016). Immunohistochemical staining with Remab6 showed highly positive staining in *Cosmc* KO tissues, but not normal tissues (Figure 4A). Immunohistochemical staining in IEC-*Cosmc* KO mice with Remab6-HRP and Remab6-Fab-HRP also showed focused, strong Tn staining in small intestine–colon–rectum sections in IEC- *Cosmc* KO mice compared to WT (Supplementary Fig. S6).

We also assessed immunohistochemical staining using human cancer cell block sections including human colorectal, breast and gastric cancer cell lines, in which Remab6 specifically stained those previously identified as being potentially Tn-positive (Figure 4B). Finally, Remab6 was screened on a large set of normal and malignant samples on tissue arrays. The results demonstrate that Remab6 stains breast, gastrointestinal, prostate, ovarian, cervical and pancreatic and pancreatic tissues of tumor origin, but rarely stained normal tissues (Figure 4C, Supplementary Fig. S7, Table IIa and IIb). In tabulating the Tn staining data using the cancer tissue array, 27 tumor tissue types were tested and 12 showed positive staining (44% of tumor tissue types tested), compared to the 30 normal tissue types tested where only 3 showed positive staining (10% of normal tissue types) (Table III). Interestingly, however, in these normal tissues, when positive, staining was only observed intracellularly, not on the cell surface, whereas malignant tissue stained both intra- and extracellularly. Intracellular staining of normal tissue represents immature glycoproteins in transit during biosynthesis where the Tn antigen is an intermediate. In addition, the extent and intensity of Tn expression were significantly greater in malignant tissues compared to normal tissue from the same organ, noting that these arrays contain multiple cell types in both normal and tumor tissues. These data demonstrate that Remab6 is specific for the Tn antigen in tumor cell surfaces and thus may be useful for detecting carcinomas.

Table IIa. FDA808k-1 multiple-organ normal tissue array, including the pathology diagnosis and results of Tn expression studies by IHC

FDA808k-1

No	Age	Sex	Organ/Anatomic Site	Pathology diagnosis	TNM[a]	Grade	Stage	Type[b]	Tn expression[c]
A1	49	M	Cerebrum	Cerebrum tissue	-	-	-	Normal	-
A2	38	F	Cerebrum	Cerebrum tissue	-	-	-	Normal	-
A3	50	F	Cerebrum	Cerebrum tissue	-	-	-	Normal	-
A4	24	F	Cerebellum	Cerebellum tissue	-	-	-	Normal	-
A5	32	M	Cerebellum	Cerebellum tissue	-	-	-	Normal	-
A6	45	M	Cerebellum	Cerebellum tissue	-	-	-	Normal	-
A7	45	M	Adrenal gland	Adrenal gland tissue	-	-	-	Normal	-
A8	27	M	Adrenal gland	Adrenal gland tissue	-	-	-	Normal	-
A9	43	M	Adrenal gland	Adrenal gland tissue	-	-	-	Normal	-
B1	45	F	Ovary	Adjacent normal ovary tissue	-	-	-	NAT	-
B2	35	F	Ovary	Adjacent normal ovary tissue	-	-	-	NAT	-
B3	64	F	Ovary	Adjacent normal ovary tissue	-	-	-	NAT	-
B4	40	F	Pancreas	Pancreas tissue	-	-	-	Normal	-
B5	21	F	Pancreas	Pancreas tissue	-	-	-	Normal	-
B6	27	M	Pancreas	Pancreas tissue	-	-	-	Normal	-
B7	41	F	Lymph node	Lymph node tissue	-	-	-	Normal	-
B8	43	M	Lymph node	Lymph node tissue	-	-	-	Normal	-
B9	35	M	Lymph node	Lymph node tissue	-	-	-	Normal	-
C1	-	-	Hypophysis	Hypophysis tissue	-	-	-	Normal	-
C2	34	M	Hypophysis	Hypophysis tissue	-	-	-	Normal	-
C3	21	F	Hypophysis	Hypophysis tissue	-	-	-	Normal	-
C4	35	M	Testis	Testis tissue	-	-	-	Normal	-
C5	65	M	Testis	Adjacent normal testis tissue	-	-	-	NAT	-
C6	74	M	Testis	Adjacent normal testis tissue	-	-	-	NAT	-
C7	22	M	Thyroid gland	Thyroid gland tissue	-	-	-	Normal	-
C8	40	F	Thyroid gland	Thyroid gland tissue	-	-	-	Normal	-
C9	35	M	Thyroid gland	Thyroid gland tissue	-	-	-	Normal	-
D1	29	F	Breast	Cancer adjacent breast tissue	-	-	-	AT	-
D2	21	F	Breast	Breast tissue	-	-	-	Normal	-
D3	35	F	Breast	Adjacent normal breast tissue	-	-	-	NAT	-
D4	38	M	Spleen	Spleen tissue	-	-	-	Normal	-
D5	21	F	Spleen	Spleen tissue	-	-	-	Normal	-
D6	23	M	Spleen	Spleen tissue	-	-	-	Normal	-
D7	34	M	Tonsil	Tonsil tissue	-	-	-	Normal	-
D8	21	F	Tonsil	Tonsil tissue	-	-	-	Normal	-
D9	45	M	Tonsil	Tonsil tissue	-	-	-	Normal	-
E1	16	M	Thymus gland	Thymus gland tissue	-	-	-	Normal	-
E2	0.7	M	Thymus gland	Adjacent normal thymus gland tissue	-	-	-	NAT	-
E3	15	F	Thymus gland	Thymus gland tissue	-	-	-	Normal	-
E4	21	F	Bone marrow	Bone marrow tissue	-	-	-	Normal	-
E5	61	F	Bone marrow	Adjacent normal bone marrow tissue	-	-	-	NAT	-
E6	70	M	Bone marrow	Adjacent normal bone marrow tissue	-	-	-	NAT	-
E7	16	F	Lung	Lung tissue	-	-	-	Normal	-
E8	30	M	Lung	Lung tissue	-	-	-	Normal	-
E9	21	F	Lung	Lung tissue	-	-	-	Normal	-
F1	35	F	Heart	Cardiac muscle tissue	-	-	-	Normal	-
F2	26	M	Heart	Cardiac muscle tissue	-	-	-	Normal	-
F3	40	M	Heart	Cardiac muscle tissue	-	-	-	Normal	-
F4	34	M	Esophagus	Esophagus tissue	-	-	-	Normal	-
F5	30	M	Esophagus	Esophagus tissue	-	-	-	Normal	-
F6	24	M	Esophagus	Esophagus tissue	-	-	-	Normal	-
F7	24	M	Stomach	Stomach tissue	-	-	-	Normal	Positive*
F8	30	M	Stomach	Stomach tissue	-	-	-	Normal	-
F9	38	M	Stomach	Stomach tissue	-	-	-	Normal	-
G1	45	M	Small intestine	Small intestine tissue	-	-	-	Normal	Positive*

(*Continued*)

Table IIa. Continued.

FDA808k-1

No	Age	Sex	Organ/Anatomic Site	Pathology diagnosis	TNM[a]	Grade	Stage	Type[b]	Tn expression[c]
G2	45	M	Small intestine	Small intestine tissue	-	-	-	Normal	Positive*
G3	21	F	Small intestine	Small intestine tissue	-	-	-	Normal	-
G4	30	M	Colon	Colon tissue	-	-	-	Normal	Positive*
G5	45	M	Colon	Colon tissue	-	-	-	Normal	-
G6	35	M	Colon	Colon tissue	-	-	-	Normal	-
G7	43	M	Liver	Liver tissue	-	-	-	Normal	-
G8	35	M	Liver	Liver tissue	-	-	-	Normal	-
G9	40	M	Liver	Liver tissue	-	-	-	Normal	-
H1	40	M	Tongue	Salivary gland tissue	-	-	-	Normal	-
H2	35	M	Tongue	Salivary gland tissue	-	-	-	Normal	-
H3	54	F	Tongue	Adjacent normal salivary gland tissue	-	-	-	NAT	-
H4	38	M	Kidney	Kidney tissue	-	-	-	Normal	-
H5	47	M	Kidney	Kidney tissue	-	-	-	Normal	-
H6	50	M	Kidney	Kidney tissue	-	-	-	Normal	-
H7	43	M	Prostate	Prostate tissue	-	-	-	Normal	-
H8	31	M	Prostate	Prostate tissue	-	-	-	Normal	-
H9	35	M	Prostate	Adjacent normal prostate tissue	-	-	-	NAT	-
H10	42	M	Adrenal gland	Pheochromocytoma (tissue marker)	-	-	-	Malig	-

[a]**TNM grading T—Primary tumor**, Tx—Primary tumor cannot be assessed, T0—No evidence of primary tumor, Tis—Carcinoma in situ; intraepithelial or invasion of lamina propria, T1—Tumor invades submucosa, T2—Tumor invades muscularis propria, T3—Tumor invades through muscularis propria into subserosa or into non-peritonealized pericolic or perirectal tissues, T4—Tumor directly invades other organs or structures and/or perforate visceral peritoneum, **N—Regional lymph nodes**, Nx—Regional lymph nodes cannot be assessed, N0—No regional lymph node metastasis, N1—Metastasis in 1 to 3 regional lymph nodes, N2—Metastasis in 4 or more regional lymph nodes, **M—Distant metastasis,** Mx—Distant metastasis cannot be assessed, M0—No distant metastasis, M1—Distant metastasis, **N—Regional lymph nodes**, Nx—Regional lymph nodes cannot be assessed, N0—No regional lymph node metastasis, N1—Metastasis in 1 to 3 regional lymph nodes, N2—Metastasis in 4 or more regional lymph nodes, **M – Distant metastasis**, Mx—Distant metastasis cannot be assessed, M0—No distant metastasis, M1—Distant metastasis
[b]**Type**, Normal—Normal tissue, NAT—Normal adjacent tissue, AT—Adjacent tissue, Malig—Malignant tissue
[c]**Tn expression**, Indicates positive or negative staining in IHC
*Intracellular staining

Table IIb. FDA808k-1 multiple-organ cancer tissue array, including the pathology diagnosis and results of Tn expression studies by IHC

FDA808k-2

No	Age	Sex	Organ/Anatomic Site	Pathology diagnosis	TNM[a]	Grade	Stage	Type[b]	Tn expression[c]
A1	48	F	Uterus	Adjacent normal endometrium tissue	-	-	-	NAT	-
A2	18	F	Uterus	Endometrium tissue	-	-	-	Normal	-
A3	41	F	Cervix	Adjacent normal endometrium tissue	-	-	-	NAT	-
A4	36	F	Cervix	Cancer adjacent cervical canals tissue	-	-	-	AT	-
A5	72	F	Cervix	Adjacent normal cervix tissue	-	-	-	NAT	-
A6	65	F	Cervix	Adjacent normal cervical canals tissue with squamous metaplasia	-	-	-	NAT	-
A7	40	M	Skeletal muscle	Skeletal muscle tissue	-	-	-	Normal	-
A8	49	F	Skeletal muscle	Adjacent normal skeletal muscle tissue	-	-	-	NAT	-
A9	50	M	Skeletal muscle	Skeletal muscle tissue	-	-	-	Normal	-
B1	34	M	Skin	Skin tissue of chest part	-	-	-	Normal	-
B2	21	M	Skin	Skin tissue	-	-	-	Normal	-
B3	35	M	Skin	Skin tissue of abdomen part	-	-	-	Normal	-

(*Continued*)

Table IIb. Continued.

FDA808k-2

No	Age	Sex	Organ/Anatomic Site	Pathology diagnosis	TNM[a]	Grade	Stage	Type[b]	Tn expression[c]
B4	23	M	Nerve	Peripheral nerve tissue	-	-	-	Normal	-
B5	25	M	Nerve	Peripheral nerve tissue	-	-	-	Normal	-
B6	50	M	Nerve	Peripheral nerve tissue	-	-	-	Normal	-
B7	33	M	Lung	Diaphragm tissue and mesothelial tissue	-	-	-	Normal	-
B8	19	M	Cardiac pericardium	Pericardium tissue and mesothelium tissue	-	-	-	Normal	-
B9	43	M	Cardiac pericardium	Diaphragm tissue and mesothelial tissue	-	-	-	Normal	-
C1	17	M	Cerebrum	Glioblastoma	-	4	-	Malig	-
C2	65	F	Cerebrum	Atypical meningioma	-	-	-	Malig	-
C3	40	F	Cerebrum	Glioblastoma	-	4	-	Malig	-
C4	39	F	Cerebrum	Oligodendroglioma	-	2	-	Malig	-
C5	62	F	Ovary	Endometrioid carcinoma	T2N0M0	3	II	Malig	Positive
C6	29	F	Ovary	Mucinous adenocarcinoma	T3N0M0	3	III	Malig	Positive
C7	16	F	Pancreas	Islet cell tumor	-	-	-	Malig	-
C8	64	M	Pancreas	Adenocarcinoma	T3N0M0	3	IIA	Malig	Positive
C9	32	M	Testis	Seminoma	T1N0M0	-	IA	Malig	-
D1	30	M	Testis	Embryonal carcinoma	T2N0M0	-	IB	Malig	-
D2	33	F	Thyroid gland	Medullary carcinoma	T3N0M0	-	II	Malig	-
D3	46	F	Thyroid gland	Papillary carcinoma	T4N0M0	-	IVA	Malig	-
D4	67	F	Breast	Intraductal carcinoma	TisN0M0	-	0	Malig	-
D5	58	F	Breast	Invasive ductal carcinoma	T3N1M0	2	IIIA	Malig	Positive
D6	42	F	Breast	Invasive ductal carcinoma	T2N1M0	3	IIB	Malig	Positive
D7	21	M	Spleen	Diffuse B-cell lymphoma	-	-	-	Malig	-
D8	61	M	Lung	Small cell undifferentiated carcinoma	T2N0M0	-	IB	Malig	-
D9	64	M	Lung	Squamous cell carcinoma	T2N0M0	3	IB	Malig	-
E1	42	M	Lung	Adenocarcinoma	T2N0M0	3	IB	Malig	-
E2	58	M	Esophagus	Squamous cell carcinoma	T3N1M0	2	IIIA	Malig	Positive
E3	63	M	Esophagus	Adenocarcinoma	T3N0M0	3	IIA	Malig	Positive
E4	73	F	Stomach	Adenocarcinoma	T2N1M0	3	IIA	Malig	Positive
E5	64	F	Small intestine	Adenocarcinoma	T4N0M0	3	IIB	Malig	Positive
E6	71	F	Small intestine	Malignant mesenchymoma	T2N0M0	-	I	Malig	-
E7	72	F	Colon	Adenocarcinoma	T4N0M0	2	IVA	Malig	Positive
E8	54	M	Colon	Mesenchymoma	T2N0M0	-	I	Malig	-
E9	36	M	Rectum	Adenocarcinoma	T2N0M0	2	I	Malig	-
F1	63	F	Rectum	Malignant mesenchymoma	T2N0M0	-	I	Malig	-
F2	55	F	Liver	Hepatocellular carcinoma	T3N0M0	2	IIA	Malig	-
F3	17	F	Liver	Hepatoblastoma	-	-	-	Malig	-
F4	60	M	Kidney	Clear cell carcinoma	T2N0M0	1	II	Malig	-
F5	80	M	Prostate	Adenocarcinoma (Gleason grade:4)	T3N0M0	3	III	Malig	Positive
F6	77	M	Prostate	Adenocarcinoma (Gleason grade:5)	T2N0M0	3	IIB	Malig	Positive
F7	56	F	Uterus	Lowly malignant leiomyosarcoma	T2N0M0	-	II	Malig	-
F8	50	F	Uterus	Endometrioid adenocarcinoma	T1bN0M0	1	IB	Malig	Positive
F9	57	F	Uterus	Clear cell carcinoma	T1bN0M0	-	IB	Malig	Positive
G1	36	F	Cervix	Squamous cell carcinoma	T1bN0M0	3	IB	Malig	Positive
G2	49	F	Cervix	Squamous cell carcinoma	T2N0M0	3	II	Malig	Positive
G3	20	F	Skeletal muscle	Embryonal rhabdomyosarc-oma of left leg	T1aN0M0	-	IA	Malig	-
G4	70	F	Rectum	Malignant melanoma	-	-	-	Malig	-
G5	85	F	Skin	Basal cell carcinoma of left face	T2N0M0	-	II	Malig	-
G6	64	M	Skin	Squamous cell carcinoma of chest wall	T3N0M0	2	III	Malig	-

(*Continued*)

Table IIb. Continued.

FDA808k-2

No	Age	Sex	Organ/Anatomic Site	Pathology diagnosis	TNM[a]	Grade	Stage	Type[b]	Tn expression[c]
G7	21	M	Nerve	Neurofibroma of back	-	-	-	Malig	-
G8	1	F	Retroperitoneum	Neuroblastoma	-	-	-	Malig	-
G9	60	M	Peritoneum	Malignant mesothelioma	T2N0M0	-	II	Malig	Positive
H1	55	M	Lymph node	Diffuse B cell lymphoma of armpit	-	-	-	Malig	-
H2	50	F	Lymph node	Diffuse B cell lymphoma of right thigh	-	-	-	Malig	-
H3	27	M	Lymph node	Mixed cell type Hodgkin's lymphoma of left groin	-	-	-	Malig	-
H4	36	M	Lymph node	Anaplastic large cell lymphoma of left groin	-	-	-	Malig	-
H5	58	F	Bladder	High grade urothelial carcinoma	T2N0M0	-	II	Malig	Positive
H6	62	M	Bladder	Leiomyosarcoma	T2N0M0	-	II	Malig	-
H7	37	F	Cartilage	Osteosarcoma of left femur lower section	T2N0M0	-	IIB	Malig	-
H8	48	F	Retroperitoneum	Highly malignant pleomorphic rhabdomysarcoma	T2N0M0	-	IIB	Malig	-
H9	60	F	Smooth muscle	Moderate malignant leiomyosarcoma of left buttock	T2N0M0	-	IIB	Malig	-
H10	42	M	Adrenal gland	Pheochromocytoma (tissue marker)	-	-	-	Malig	-

[a]**TNM grading**, **T—Primary tumor**, Tx—Primary tumor cannot be assessed, T0—No evidence of primary tumor, Tis—Carcinoma in situ; intraepithelial or invasion of lamina propria, T1—Tumor invades submucosa, T2—Tumor invades muscularis propria, T3—Tumor invades through muscularis propria into subserosa or into non-peritonealized pericolic or perirectal tissues, T4—Tumor directly invades other organs or structures and/or perforate visceral peritoneum, **N—Regional lymph nodes**, Nx—Regional lymph nodes cannot be assessed, N0—No regional lymph node metastasis, N1—Metastasis in 1 to 3 regional lymph nodes, N2—Metastasis in 4 or more regional lymph nodes, **M—Distant metastasis**, Mx—Distant metastasis cannot be assessed, M0—No distant metastasis, M1—Distant metastasis, **N—Regional lymph nodes**, Nx—Regional lymph nodes cannot be assessed, N0—No regional lymph node metastasis, N1—Metastasis in 1 to 3 regional lymph nodes, N2—Metastasis in 4 or more regional lymph nodes, **M—Distant metastasis**, Mx—Distant metastasis cannot be assessed, M0—No distant metastasis, M1—Distant metastasis

[b]**Type**, Normal—Normal tissue, NAT—Normal adjacent tissue, AT—Adjacent tissue, Malig—Malignant tissue

[c]**Tn expression**, Indicates positive or negative staining in IHC

*Intracellular staining

Table III. Summary of Tn staining in normal and cancer tissue arrays

Tissue	Malignant	Normal	Tissue	Malignant	Normal
Cerebrum	0/4	0/3	Esophagus	2/2	0/3
Cerebellum	-	0/3	Stomach	1/1	1/3*
Hypophysis	-	0/3	Small intestine	1/2	2/3*
Nerve	0/1	0/3	Colon	1/2	1/3*
Tongue	-	0/3	Rectum	0/2	-
Tonsil	-	0/3	Kidney	0/1	0/3
Cartilage	0/1	-	Adrenal gland	0/2	0/3
Thyroid	0/2	0/3	Bone marrow	-	0/3
Thymus	-	0/3	Prostate	2/2	0/3
Heart	-	0/3	Bladder	1/2	-
Cardiac pericardium	-	0/2	Testis	0/2	0/3
Lymph node	0/4	0/3	Ovarian	2/2	0/3
Lung	0/3	0/3	Uterus	2/3	0/1
Breast	2/3	0/3	Cervix	2/2	0/3
Liver	0/2	0/3	Peritoneum	1/3	-
Spleen	0/1	0/3	Skin	0/3	0/3
Pancreas	1/2	0/3	Skeletal muscle	0/1	0/3
			Smooth muscle	0/1	-
			* Intracellular staining		

A

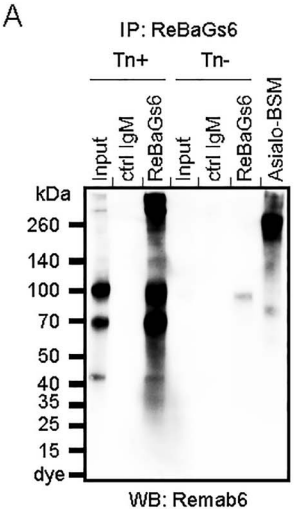

B

No	Entry name	Accession No	Protein name	Number of peptide spectral matches	Multiple Tn	Novel O-glycoproteins
1	APOE	P02649	Apolipoprotein E	28	Yes	Known
2	MUC16	Q8WXI7	Mucin-16	26	Yes	Known
3	APP	P05067	Amyloid beta A4	23	Yes	Known
4	AGRN	O00468	Agrin	19	Yes	Known
5	CD44	P16070	CD44 antigen	18	Yes	Known
6	TGFB2	P61812	Transforming growth factor beta receptor 2	16	Yes	Novel
7	SLC2A12	Q8TD20	Solute carrier family 2 member 12	14	Yes	Novel
8	NID2	Q14112	Nidogen-2	14	Yes	Novel
9	CALU	Q43852	Calumenin	12	Yes	Novel
10	S1PR1	P21453	Sphingosine-1-phosphate receptor 1	11	Yes	Novel
11	MUC13	Q9H3R2	Mucin-13	9	Yes	Novel
12	ITA5	P08648	Integrin alpha-5	6	Yes	Known

Fig. 5. LC-MS analysis to identify Tn-containing glycoproteins in colorectal carcinoma cell line. ***(A)*** Immunoprecipitated glycoproteins with ReBaGs6 in Colo205 Simple Cell line (Tn-positive) were analyzed by western blot using Remab6. ***(B)*** The numbers of Tn-positive glycoproteins were identified by LC/ESI-MS/MS analysis using immunoprecipitates with ReBaGs6 in the Colo205 Simple Cell line (Tn-positive).

Table IV. Identification of peptide sequences by LC/ESI-MS/MS

No.	Entry name	Peptide/glycopeptide sequence #1	Peptide/glycopeptide sequence #2	Peptide/glycopeptide sequence #3
1	APOE	ALMDET* MKELK	LRARMEEMGS* RT* R	S* WFEPLVEDMQRQWAGLVEK
2	MUC16	TEALSLGRT* ST* PGPAQSTIS	DT* FNDSAAPQST* TWPETSPR	ISTSAPLSSS* AS* VLDNK
3	APP	LALENY* IT* ALQAVPPRPR	FLHQERMDVCETHLHWHT* VAKETCSEK	PAADRGLTTR[a]
4	AGRN	TTAAPTTRRPPT* T* APSRVPGR	TTAAPTTRR[a]	KDFRSVR[a]
5	CD44	KPS* GLNGEAS* KS* QEMVHLVNK	SQEMVHLVNK[a]	RMDMDSSHSITLQPT* ANPNTGLVEDLDR
6	TGFB2	LSSTWET* GK	EHPCVES* MK	IFPY* EEY* ASWKTEK
7	SLC2A12	SS* LM** PLR	GCS* LEQISMELAKVNY* VKNNICFMSH-HQEELVPK	Y*MFGLVIPLGVLQAIAMY FLPPS*PRFLVMKGQEGAASK
8	NID2	KALEGLQY* PFAVT* SYGK	IEVAKLDGT* QR	IESALLDGSER[a]
9	CALU	MDLRQFLMCLSLCTAFALS* KPT* EK	IDGDKDGFVT* VDELKDWIK	TFDQLTPEESKER[a]
10	S1PR1	YIT* MLK	IMS* CCK	T* CDILFR
11	MUC13	HS* MAYQDLHSEITS* LFKDVF	CAFGY* S* GLDCKDK	STGFTNLGAEGSVFPK[a]
12	ITA5	ERQVAT* AVQWT* K	HPGNFSS* LS* CDY* FAVNQSR	RSLPYGTAMEK[a]

*GalNAc on serine, threonine or tyrosine; **Oxidation on methionine; [a]Not identified site-specific GalNAcylation

Identification of Tn-containing glycoproteins in colorectal cancer cell line by LC/ESI-MS/MS

We sought to use ReBaGs6 to identify Tn-containing glycoproteins that might be useful in analyses for biomarkers, as well as to explore potential mechanisms by which Tn antigen may be involved in tumor progression. To this end, we examined the glycoproteins recognized by ReBaGs6 in Colo205 Simple Cells (Tn-positive) engineered by deletion of the *Cosmc* gene from parental Colo205 cells. ReBaGs6 was conjugated to UltraLink beads and the conjugate was used for immunoprecipitation experiments using Colo205 Simple Cell (Tn-positive) lysates. A number of Tn-containing glycoproteins were captured, as identified by subsequent western blot using Remab6 (Figure 5A). As a control, we also examined glycopeptide sequences from Asialo-BSM. Several Tn-containing peptide sequences were identified from Asialo-BSM under multiple higher collision dissociation (HCD) energies (Supplementary Fig. S8). The monoisotopic precursor isotopic pattern was matched against the theoretical peptide for several peptide spectral matches identified via decoy database search with SEQUEST.

With success in these control studies on Asialo-BSM, we used similar instrument settings to identify tryptic glycopeptides using immunoprecipitates in Colo205 Simple Cells (Tn-positive). Using this approach, we identified several unique glycoproteins and unique peptide sequences with GalNAc modifications from the Colo205 Simple Cell line (Tn-positive), but not the control Tn-negative Colo205 cell line (Figure 5B). GO annotation of the identified glycopeptides is specific to either membrane glycoproteins or their secreted counterparts, and a number of such tryptic glycopeptides containing GalNAc are listed (Table IV). Interestingly, we also observed GalNAc on tyrosine residues in several glycopeptides. This modification was observed in a recent study (Vakhrushev et al. 2013), but there have been few reports of its presence. These Tn-containing glycoproteins also included several sites predicted to be O-glycosylated, but not yet proven by chemical analysis, such as LC-MS/MS or western blot analysis. Together, our results indicate that both Remab6 and ReBaGs6 do not require specific amino acid backbones for recognition and that these antibodies specifically recognize the Tn antigen on several unique glycoproteins in Colo205 cells. These unique glycoproteins will be useful in future biomarker studies.

Discussion

Here we have presented our development of a novel set of recombinant anti-Tn monoclonal antibodies, human IgG1 Remab6 and murine IgM ReBaGs6. These antibodies are specific for the Tn antigen in glycoproteins and do not simply recognize terminal α-linked GalNAc residues, as may occur in BGA and other types of glycans. Importantly, the engineered antibodies do not recognize the Tn antigen present in the hinge region of IgA1. Furthermore, in normal murine tissues we did not observe binding of Remab6, whereas in murine tissues from mice engineered to lack Cosmc and express the Tn antigen, we observed extensive staining. The recombinant anti-Tn antibodies also allowed identification of novel Tn-positive glycoproteins in a human tumor cell line.

Anti-glycan antibodies

Alteration of glycan structures in cancer is a common feature and has led to the development of glycoprotein-based biomarkers, including glycan- or glycoprotein-targeted antibodies, such as CA19-9, CA15-3, CA125 and CA72-4 (Chen et al. 2018). Several antibodies against those targets have been developed, but not all glycan structures are equally immunogenic, biasing the production of antibodies. Glycan determinants recognized by antibodies and other glycan-binding proteins (GBPs) minimally contain two to six monosaccharides, limiting the generation of mAbs against single monosaccharides, such as GalNAc (Cummings 2009). From the traditional immunology viewpoint, glycans alone elicit T cell-independent immunity, whereas glycopeptides elicit glycopeptide–MHC-II interactions for presentation and T-cell dependency (Singh et al. 2011). Interestingly, while some Tn-containing MUC1 glycopeptides elicit T cell-dependent immune response, other glycopeptides with identical aglycon backbones but distinct Tn attachment sites do not, despite being endocytosed by dendritic cells, suggesting that the selection of glycosylation sites is a critical key for immunogen design (Vlad et al. 2002).

This complexity in the immune response has prompted many laboratories to generate monoclonal antibodies against the Tn antigen by immunizing with whole cancer cells (Springer et al. 1988; Bigbee et al. 1990; King et al. 1991; Brooks et al. 2010; Welinder et al. 2011; Blixt et al. 2012), membrane proteins/cultured supernatants from cancer cells (Hirohashi et al. 1985; Springer et al. 1988; Takahashi et al. 1988; Numata et al. 1990; King et al. 1991; Huang et al. 1992; Osinaga et al. 2000; Ando et al. 2008), Tn-linker molecules and synthesized Tn glycopeptides as an immunogen (Longenecker et al. 1987; Thurnher et al. 1993; Reis et al. 1998; Sorensen et al. 2006; Danussi et al. 2009; Mazal et al. 2013; Naito et al. 2017; Persson et al. 2017) and phage display (Kubota et al. 2010; Sakai et al. 2010). Some of these anti-Tn antibodies have been demonstrated to inhibit the growth of colon and breast cancer cell lines (Morita et al. 2009), tumor rejection (Hubert et al. 2011) and anti-tumor activity in vitro and in vivo (Avichezer et al. 1997; Ando et al. 2008; Kubota et al. 2010; Welinder et al. 2011; Sedlik et al. 2016) and used for in vivo imaging (Nakamoto et al. 1998; Danussi et al. 2009). However, monoclonal antibodies to the Tn antigen are notably difficult to generate and are expensive to produce, and their specificities are often not well characterized, especially in regard to whether the anti-Tn antibodies recognize the Tn-positive IgA1 glycoform (Lehoux et al. 2014). This latter feature is generally not tested nor appreciated. Therefore, our engineered antibodies that do not recognize IgA1 provide a valuable alternative that can be reproducibly made on a large scale and retain the fine specificity that we have characterized. Our previous study has demonstrated that Tn-modified glycopeptides show drastic conformational changes, which might give rise to unpredicted immunogenic epitopes (Borgert et al. 2012). As both Remab6 and ReBaGs6 do not show cross reactivity to Tn antigen on IgA1 and can recognize tumor cell-expressed glycoproteins, the results suggest that these antibodies could be promising therapeutics and diagnostics in cancer.

Remab6 is specific for Tn antigen on multiple unique glycoproteins in cancer

Remab6 was functional in multiple types of assays and provided clues to understand the mechanisms by which Tn-containing glycoproteins could be involved in cancer progression by LC/ESI-MS/MS analysis with immunoprecipitation (Figure 5). Consistent with prior studies, some of the Tn-containing glycoproteins we identified have been seen previously using VVA lectin chromatography with a *Cosmc* knockout cell line and LC-MS^n analysis (Radhakrishnan et al. 2014; Campos et al. 2015), and the established GlycoDomainViewer database (Joshi et al. 2018). We also identified several glycoproteins, such as APOE, MUC16, AGRN, CD44 and ITA5, which were identified using VVA lectin chromatography (Vakhrushev et al. 2013). In our study, however, we also identified several additional and novel Tn-containing glycoproteins (Figure 5B, Table IV). Among the novel proteins in the list, the unique glycopeptides in APP (Amyloid beta A4) were first identified in our study, although APP was identified as an O-glycosylated glycoprotein in a prior study (Steentoft et al. 2011). Among the novel O-glycosylated glycoproteins we identified are TGFβ2, SLC2A12, NID2, CALU, S1PR1 and MUC13, all of which have suggested roles in colorectal cancer.

For example, TGFβ2 is associated with the hypoxic tumor microenvironment to promote cancer cell stemness and chemoresistance in colorectal carcinoma (Tang et al. 2018). SLC2A12 (GLUT12) is correlated with the androgen receptor (AR) in multiple clinical cohorts and is required for maximal androgen-mediated glucose uptake to promote cell growth in prostate cancer (White et al. 2018). NID2 is characterized as a tumor suppressor gene and serves to maintain the extracellular matrix environment, to suppress liver metastasis by regulating EGFR/Akt and Integrin/FAK/PLCc pathways (Chai et al. 2016). CALU is an extracellular molecule

and stabilizes fibulin-1 and regulates cell migration via the ERK1/2 signaling pathway in hepatocellular and pancreatic carcinomas (Wang et al. 2015). S1PR1 is an important factor in promoting metastasis via the tumor microenvironment in multiple carcinomas (Rostami et al. 2019). MUC13 is known to play a protective role in colorectal cancer by activating the NF-κB pathway, whereas another well-known mucin MUC16 plays an opposite role in extending tumor metastasis (Sheng et al. 2017).

Of note, tyrosine O-GalNAcylation has been reported for a handful of glycopeptides in a recent study (Vakhrushev et al. 2013). In addition to the more well-known PTM identifications on tyrosine such as phosphorylation and sulfation, tyrosine glycosylation is typically not considered for data analysis as commonly as serine and threonine, as is evident from our report and others that routine mining of tyrosine GalNAc residue should be considered for all future MS analyses. This tyrosine GalNAcylation could be orchestrated with serine or threonine GalNAcylation to affect oncogenic properties, but that remains to be studied. Thus, using the specific anti-Tn antibody in immunoprecipitation studies, we identified both several novel O-glycosylated glycoproteins and novel tyrosine O-GalNAcylation sites on peptides.

Overall, the results demonstrate that Remab6 does not recognize any particular amino acid backbone, yet the peptide expression is required for antigen expression and some peptide presentations may not be recognized by Remab6. The inhibition data indicate that Asialo-BSM is a better inhibitor of BaGs6, compared to VVA, and the monosaccharide GalNAc only weakly inhibits BaGs6 (Supplementary Fig. S1B). This suggests that there is little cross-reactivity with other glycan structures terminating in α-linked GalNAc, in contrast to VVA and HPA, which simply recognize terminal α-linked GalNAc-R residues. This is in line with the requirement for multiple clustered sites (Figure 2B), and as shown in previous binding studies with BaGs6 (Borgert et al. 2012), and the sequence requirements suggest the peptide backbone plays a role or is an important factor for spatially orienting the sugar residues. To date, several groups have demonstrated that Tn-containing glycoproteins modulate cell proliferation, invasion, metastatic potential and immunosurveillance in some types of cancers (Wagner et al. 2007; Kanoh et al. 2008; Park et al. 2010; Park et al. 2011; Taniuchi et al. 2011; Wu et al. 2011; Saeland et al. 2012; Matsumoto et al. 2013; Ho et al. 2014; Hofmann et al. 2015; Song et al. 2015; Niang et al. 2016; Song et al. 2016; Lin et al. 2017). The surface expression of Tn-positive glycoproteins in tumor cells suggests that Remab6 could exhibit anti-tumor efficacy.

Remab6 is useful as a diagnostic biomarker in several types of cancer, as well as a potential targeted therapy

Remab6 has potential as a diagnostic marker to detect Tn-carrying mucins in the serum or feces of cancer patients. Our results with a human cancer tissue array indicate that Remab6 could be useful for the detection of Tn-expressing human carcinomas using biopsies with patients or CT/MRI imaging with limited off-target effects, since there was little reactivity on the surface of normal tissues (Figure 4C, Supplementary Fig. S7). Using the recombinant antibodies described here, we can imagine several therapeutic applications, including (1) antibody-drug conjugate (ADC) technique, (2) CAR-T cell engineering, (3) antibody-dependent cellular cytotoxicity/complement-dependent cytotoxicity-based immunotherapy and (4) bispecific antibody (bsAb) technology. Recently, ADC with Chi-Tn, a mouse/human chimeric antibody for Tn antigen, showed anti-tumor efficacy when the antibody was internalized, and the cytotoxic drug is active in early and recycling endosomes (Sedlik et al. 2016). MUC1-Tn engineering CAR-T cells have been established and showed a potent antitumor efficacy in xenograft models of T cell leukemia and pancreatic cancer (Posey et al. 2016). These data indicate that Remab6 is a promising tool for detection, diagnosis and therapeutic treatment in human carcinomas.

Materials and methods

Cell culture

Human colorectal carcinoma LSC and LSB cells were a kind gift from Dr. Steven Itzkowitz (Mount Sinai School of Medicine) (Brockhausen et al. 1998). Human colorectal carcinoma LS174T, and acute T cell leukemia Jurkat cells, which carry a *Cosmc* mutation and express the Tn antigen (Ju and Cummings 2002), were purchased from American Type Culture Collection (ATCC). Tn-positive and -negative populations in LS174T cells were isolated previously (Ju et al. 2008). The human colon adenocarcinoma Colo205 cell line, human breast adenocarcinoma MDA-MB-231 cell line, human gastric adenocarcinoma MKN-45 cell line and the corresponding Tn-positive Simple Cells of each cell line, which were generated by deletion of the *Cosmc* gene, were a kind gift from Dr. Henrik Clausen (University of Copenhagen) (Steentoft et al. 2013). LSC, LSB, LS174T and MDA-MB-231 cells were cultured in Dulbecco's Modified Eagle's Medium (DMEM) (Corning®) supplemented with 10% (vol/vol) fetal bovine serum and 200 units/mL penicillin–streptomycin at 37°C and 5% CO_2. Jurkat, Colo205 and MKN-45 cells were cultured in RPMI 1640 medium (Corning®) supplemented with 10% (vol/vol) fetal bovine serum and 200 units/mL penicillin–streptomycin at 37°C and 5% CO_2.

Preparation of Asialo-BSM affinity resin

Bovine submaxillary mucin (BSM) (Sigma) was coupled with UltraLink™ Biosupport resin (Thermo Fisher Scientific) as previously described (Ju et al. 2002a). The coupled BSM beads were desialylated by the addition of 50 mU of *Arthrobacter ureafaciens* neuraminidase (Roche) in 50 mM sodium acetate (pH 5.0) for 1 h at 37°C. The resin was washed with PBS three times, and the beads were collected and desialylated once more to completely remove the sialic acid, to generate desialylated BSM (Asialo-BSM) beads.

Immunofluorescence of Asialo-BSM beads

BSM beads, Asialo-BSM beads or beads alone were incubated with ascites fluid containing the anti-Tn IgM BaGs6 (diluted 1:100 in PBS) or mouse anti-STn mAb (SCBT, B72.3, diluted to 1 µg/mL in PBS) for 1 h on ice. The beads were washed three times with 1 M NaCl and incubated with Alexa Fluor® 488-goat anti-mouse IgM or IgG secondary (Thermo Fisher Scientific) at 1:400 dilution in PBS for 1 h on ice in the dark. The beads were washed three times with PBS and analyzed using a microscope (Zeiss; Axio Imager M1). Isotype antibodies, mouse IgM and IgG, were used as controls, for the ascites and anti-STn mAb, respectively.

Affinity purification and sequencing of anti-Tn antibody from mouse ascites

An ascites fluid containing BaGs6 (8 mg/mL), a murine IgM monoclonal antibody, was a kind gift from the late Georg Springer, but

no hybridoma exists. To purify BaGs6, the ascites fluid was mixed with Asialo-BSM beads and rotated overnight in a cold room. After the mixture was washed six times with 1 M NaCl on the column, bound material was eluted by 0.1 M glycine-NaOH (pH 10.5) and neutralized with 1 M glycine-HCl (pH 2.7). The concentration of purified mAb was determined by Pierce™ BCA assay kit (Thermo Fisher Scientific) following the manufacturer's instructions with BSA as a standard. Each fraction was analyzed on SDS-PAGE (GenScript) and stained with Coomassie. The affinity-purified antibody was de novo sequenced by LC-MS/MS^n with multiple proteolytic approaches at Digital Proteomics Inc. (San Diego, CA). Using this information, we then constructed genes encoding the heavy and light chain and complementarity-determining regions (CDR) with appropriate proprietary amino acid substitutions. For large-scale production, ReBaGs6 was outsourced to LakePharma Inc. (San Carlo, CA) for production and purification.

Cloning and expression of recombinant human chimeric anti-Tn mAb (Remab6, hIgG1)

DNA fragments engineered to represent the heavy mu chain and kappa light chain-variable domains in BaGs6 were synthesized by Genewiz, Inc. (South Plainfield, NJ) into the pUC57 vector. Synthetic DNA fragments representing aspects of the variable domains of BaGs6 were subcloned into pFUSEss-CHIg-hG1 and pFUSE2ss-CLIg-hk vectors (InvivoGen), respectively. HEK293 Freestyle cells were grown to a density of 2.5×10^6 cells/mL in Freestyle Expression Medium (Life Technologies) in suspension on a platform shaker in a humidified 37°C incubator. Before transfection, the cells were harvested at 300*xg* for 10 min and resuspended in fresh medium. Then, the cells were co-transfected with 3 µg/mL in total of plasmid vectors expressing heavy chain and light chain (2:3 ratio), and with 9 µL/mL of polyethylenimine (PEI) at a final concentration of 0.5 µg DNAs or PEI/µL media in transfection solution. After 24 h, the cells were diluted 1:1 with fresh media supplemented with valproic acid (Sigma-Aldrich) at a final concentration of 2.2 mM. After 7 d post-transfection, cultured supernatant was collected after centrifugation at 300 *x g* for 10 min.

Purification of Remab6 using Protein A affinity chromatography

The culture supernatant was applied to a Protein A-Agarose column (Roche) equilibrated with 100 mM Tris, pH 8.0. After the column was washed with 100 mM Tris–HCl, pH 8.0, once, and 10 mM Tris-HCl, pH 8.0, twice, Remab6 was eluted by 0.1 M glycine–HCl, pH 2.7, and neutralized with 1 M Tris–HCl, pH 9. The concentration of purified Remab6 was determined with the Pierce™ BCA assay kit.

Tn glycopeptide microarray and CFG microarray

The Tn glycopeptide microarray was prepared as previously described (Borgert et al. 2012). The list of glycopeptides printed on the microarray is given in Table I. The Consortium for Functional Glycomics (CFG) glycan microarray version 5.0 was used (www.functionalglycomics.org) (Heimburg-Molinaro et al. 2011). Briefly, Remab6 (diluted to 5 µg/mL), ReBaGs6 (diluted to 20 and 2 µg/mL) or mouse ascites (diluted 1:200) in TSM binding buffer (20 mM Tris–HCl, pH 7.4, 150 mM NaCl, 2 mM $CaCl_2$, 2 mM $MgCl_2$, with 1% BSA and 0.05% Tween-20) were added to the array slides for 1 h at RT. Slides were washed four times with TSM wash buffer 1 (20 mM Tris–HCl, pH 7.4, 150 mM NaCl, 2 mM $CaCl_2$, 2 mM $MgCl_2$ and 0.05% Tween-20) and washed four times with TSM wash buffer 2 (20 mM Tris–HCl, pH 7.4, 150 mM NaCl, 2 mM $CaCl_2$ and 2 mM $MgCl_2$). Alexa Fluor® 488-labeled goat anti-human IgG or goat anti-mouse IgM secondary (diluted to 5 µg/mL) were used for detection. After washing as above, slides were washed once in water and dried before being read on a GenePix® 4300A microarray scanner (Molecular Devices). Images were analyzed with quantitation software (GenePix® Pro Microarray Analysis Software Ver. 7, Molecular Devices).

Preparation of remodeled glycopeptide arrays—STn and T glycopeptide array

The STn glycopeptide array was generated by incubating the Tn glycopeptide microarray slides (ID1–8) with the sialyltransferase, ST6GalNAc-I, and 1 mM of 5′-biotinylated CMP-Neu5Ac (Chemily, LLC, custom order) in reaction buffer (150 mM NaCl, 20 mM cacodylate, pH 6.8, 10 mM $CaCl_2$, 10 mM $MgCl_2$, 10 mM $MnCl_2$ and 0.05% Tween-20) at 37°C overnight. Slides were washed four times with TSM wash buffer 1 and TSM wash buffer 2 before use. The T glycopeptide array was generated by incubating the Tn glycopeptide microarray slide with T-synthase with 1 mM of UDP-Gal in reaction buffer at 37°C overnight. Slides were washed four times with TSM wash buffer 1 and TSM wash buffer 2, and microarrays were probed with Remab6.

Preparation of IgA1 from *Cosmc*KO Dakiki cells and cell extracts

*Cosmc*KO Dakiki cells were generated using the CRISPR/Cas9 system, which allowed us to delete the functional *Cosmc* gene on the X-chromosome. Purification of IgA1 from Dakiki cells was previously described (Lehoux et al. 2014). For cell extracts, approximately, 5×10^6 cells were harvested and lysed with 500 µL of lysis buffer (150 mM NaCl, 20 mM Tris–HCl, pH 7.5, 2.5 mM sodium pyrophosphate, 1 mM Na_2EDTA, 1 mM EGTA, 1 mM β-glycerophosphate, 1 mM sodium orthovanadate and 1% Triton X-100) containing protease inhibitors (Roche, cOmplete™, Mini Protease Inhibitor Cocktail). After sonication, cell extract was collected from the supernatant after centrifugation at 15,000 rpm for 10 min.

Western and lectin blots

The protein concentration in purified IgA1 and cell extracts was determined by Pierce BCA kit. Asialo-BSM was prepared from BSM with neuraminidases as described in "Preparation of Asialo-BSM affinity resin". Proteins (purified IgA; 0.3 µg/lane, cell extracts; 30 µg/lane, and Asialo-BSM; 2.5 µg/lane) were analyzed on SDS-PAGE gel (GenScript) and transferred to a nitrocellulose membrane (Thermo Fisher Scientific). After blocking with 5% (w/vol) BSA in TBS + 0.05% Tween-20 (TTBS) for 1 h at RT, western and lectin blots were analyzed with Remab6 and ReBaGs6 (diluted at 5 µg/mL, 2 µg/mL in TTBS, respectively), biotinylated VVA (Vector Laboratories, diluted at 1 µg/mL in TTBS) or horseradish peroxidase (HRP)-labeled goat anti-human IgA (alpha) antibody (Sigma, diluted at 1:5000 in TTBS) as a primary staining. Secondary detection was performed with HRP-labeled goat anti-human IgG antibody, goat anti-mouse IgM antibody (KPL) and streptavidin-HRP (Vector Laboratories) at 1:5000 dilution in TTBS, using SuperSignal™ West Pico Chemiluminescent Substrate (Thermo Fisher Scientific), then analyzed on an Amersham™ Imager 600 (GE Healthcare Life Sciences).

Binding and inhibition assays

Asialo-BSM (0.5 μg/well) was immobilized with immobilization buffer ($NaHCO_3/Na_2CO_3$, pH 9.6) in a 96-well plate (Thermo Fisher Scientific, PolySorp) overnight at 4°C. The plate was washed with TTBS and added with 5% (w/v) BSA in TTBS for 1 h at RT. The plate was incubated with a serial dilution of ReBaGs6 and Remab6 and biotinylated VVA in TTBS for 1 h at RT. The plate was washed with TTBS and incubated with Alexa Fluor® 488-labeled goat anti-mouse IgM, goat anti-human IgG or streptavidin at 1:1000 dilution in TTBS for 1 h at RT in the dark. The plate was washed with TTBS and read on an ImageXpress® Pico (Molecular Devices). Affinity constant was calculated with GraphPad Prism 6.0 (GraphPad Software, Inc.). For inhibition assay, ReBaGs6, Remab6 and biotinylated VVA were preincubated with 100 mM GalNAc or 100 mM GlcNAc for 30 min at RT.

Flow cytometry

Cells were collected and washed with cold PBS twice, then 5×10^5 cells were transferred into tubes. Cells were treated with 50 mU of neuraminidases in PBS for 1 h at 37°C, then washed, and incubated with 100 μL of Remab6 (diluted to 5 μg/mL in PBS) or mouse anti-STn mAb (diluted to 1 μg/mL in PBS) for 1 h on ice. For controls, cells were incubated with 100 μL of human IgG or mouse IgG (SouthernBiotech) for 1 h on ice. Cells were washed twice with cold PBS, and incubated with 100 μL of Alexa Fluor® 488-labeled goat anti-human IgG or goat anti-mouse IgG (Thermo Fisher Scientific) at 1:400 dilution in PBS for 1 h on ice in the dark. Cells were washed twice with cold PBS, resuspended in 500 μL of PBS and analyzed on a flow cytometer (FACSCalibur™, Becton Dickinson).

Confocal microscope imaging

For immunofluorescence with cultured cells, cells were fixed with 4% (vol/vol) paraformaldehyde (PFA) in PBS for 30 min on ice, permeabilized with 0.1% (vol/vol) Triton X-100 in PBS for 10 min on ice. After blocking with 5% (w/vol) BSA in PBS for 1 h at 4°C, cells were co-stained with Remab6 (diluted to 5 μg/mL in PBS + 0.5% BSA) and rabbit anti-Calnexin mAb (CST, 1:100 dilution in PBS + 0.5% BSA), rabbit anti-Giantin pAb (Abcam, 1:500 dilution in PBS + 0.5% BSA) or sheep anti-TGN46 pAb (Bio-Rad, 1:500 dilution in PBS + 0.5% BSA) for 1 h at 4°C. Cells were washed three times with PBS and co-stained with Alexa Fluor® 488-labeled goat anti-human IgG and Alexa Fluor® 568-labeled goat anti-rabbit IgG or Alexa Fluor® 568-labeled donkey anti-sheep IgG secondaries (Thermo Fisher Scientific) at 1:400 dilution in PBS + 0.5% BSA for 1 h at 4°C in the dark. Cells were washed three times with PBS and stained with DAPI for 10 min at RT in the dark, then cells were analyzed by confocal microscope (Zeiss; Axioimager Z1). Isotype antibodies (human IgG, rabbit IgG or sheep IgG) (Southern Biotech) were co-stained as controls.

Immunoprecipitation and western blot

Cell extracts were prepared as described in "Preparation of IgA1 from *Cosmc*-KO Dakiki cells and cell extracts". Cell extracts from the Colo205 simple cell line (Tn-positive) were immunoprecipitated with ReBaGs6 or isotype control mouse IgM-conjugated with UltraLink™ beads overnight at 4°C. Immunoprecipitates were analyzed by western blot as described in "Western and lectin blots". Remab6 (2 μg/mL in TTBS) and horseradish peroxidase (HRP) labeled with goat anti-human IgG antibody (KPL) at 1:5000 dilution in TTBS were used for detection.

LC/ESI-MS/MS mass spectrometry analysis

Immunoprecipitates in Coomassie-stained gel were de-stained and washed with a series of three washing buffers (50 mM ammonium bicarbonate, 50% acetonitrile and 80% acetonitrile). The bound proteins were reduced with 1 mL of 40 mM dithiothreitol for 25 min at 56°C. The pieces of gel were rinsed with 1 mL of 50 mM ammonium bicarbonate buffer, and the reduced proteins were alkylated with 1 mL of 50 mM iodoacetamide for 30 min at 25°C in the dark with gentle mixing. Iodoacetamide was discarded, and the gel-bound proteins were digested with 0.5 mL of trypsin (Promega, diluted at 20 ng/μL) in 50 mM ammonium bicarbonate buffer at 37°C with gentle mixing for 12 h. After digestion, the tryptic fractions were collected, and the gels were washed with 50 mM ammonium bicarbonate to collect any remaining tryptic peptides. The eluents containing tryptic peptides were dried using a Speed-Vac apparatus (Thermo Fisher Scientific) and stored at 4°C prior to mass spectrometric analysis. The dried samples were dissolved with 20 μL of 0.1% formic acid/water. Two microliters of each sample was analyzed by LC/ESI-MS/MS using a Fusion™ Lumos™ (Thermo Fisher) mass spectrometer (MS) with a Dionex LC system using data-dependent acquisition with dynamic exclusion (DE = 1) settings. The data-dependent acquisition settings were a top 12 higher energy collision-induced dissociation (HCD) for the Fusion™ Lumos™ MS. The resolving power for Fusion™ Lumos™ was set at 120,000 for the full MS scan and 35,000 for the MS/MS scan at m/z 200. LC/ESI-MS/MS analyses were conducted using a C18 column (75 μm × 150 μm). The mobile phases for the reversed-phase chromatography were (A) 0.1% HCOOH/water, and (B) 0.1% HCOOH in acetonitrile. A four-step linear gradient was used for the LC separation (2% to 30% B in the first 47 min, followed by 80% B in the next 1 min and holding at 80% B for 12 min). The SEQUEST algorithm was used to identify peptides from the resulting MS/MS spectra by searching against the combined human protein database (22,673 proteins in total) extracted from Swiss-Prot (version 57) using taxonomy "*Homo sapiens*" using Proteome Discoverer™ (Thermo Scientific, version 1.4). Searching parameters for parent and fragment ion tolerances were set as 15 ppm and 30 mmu for the Fusion™ Lumos™. Other parameters were used as a fixed modification of carbamidomethylation (C), variable modifications of acetylation (K), HexNAc (S, T) and oxidation (Met). Trypsin was set as the protease with a maximum of two missed cleavages. Raw files were searched against top 6 O-glycans using Byonic™ (Bern et al. 2007) with a peptide tolerance of 15 ppm and an MS/MS tolerance of 20 ppm for HCD data and the carbamidomethylated cysteine as fixed modification and oxidation of methionine and acetylation (K) as variable modifications. Byonic™ scoring gives an indication of whether modifications are confidently localized.

Immunohistochemical staining in IEC-Cosmc KO mice sections and human cancer cell blocks

Intestines from WT and IEC-*Cosmc* KO mice were dissected and prepared by Swiss-roll as previously described (Kudelka et al. 2016), following all approved IACUC protocols and guidelines. Formalin-fixed paraffin-embedded (FFPE) sections were deparaffinized and retrieved by boiling for 10 min in retrieval buffer (10 mM citrate, pH 6). After cooling down, sections were treated with 0.3% H_2O_2 for 10 min and blocked with 5% (vol/vol) goat serum (Gibco) in

TBS for 1 h at RT. Sections were stained with Remab6 (5 µg/mL in TBS + 0.1% Triton X-100, TBSTx) overnight at 4°C. HRP-labeled goat anti-human IgG antibody (KPL) at 1:400 dilution in TBSTx was added for 1 h at RT, then staining was visualized using an AEC single solution (Invitrogen), which generates a brownish-red deposit where binding occurs in the tissue. Nuclear staining was performed with hematoxylin. Images were analyzed by microscope (Zeiss; Axioimager M1). Isotype human IgG was used as a control.

For human cancer cell block sections, harvested cells were collected and suspended in 10 mL of 10% neutral buffered formalin (Midland Scientific Inc.) overnight at RT. Cell pellets were suspended in 1% warm agarose solution and added to respective Eppendorf tubes with agar plug. After hardening of the agar for 15 min, agar with cells was fixed again in 10% neutral buffered formalin overnight at 4°C. Agar with cells was extruded into the immersed cassette by cutting off the bottom of the tube with a razor blade, then paraffinized.

Preparation of Remab6-Fab and conjugation with HRP

Remab6 was cleaved with papain enzyme and prepared following the manufacturer's instructions (Thermo Fisher Scientific). Conjugation with HRP to Remab6-Fab was prepared following the manufacturer's instructions (Abcam). Remab6-Fab-HRP binding to IEC-*Cosmc* KO and WT tissues was assessed, and as a control, isotype-matched human IgG-Fab-HRP was prepared and used for the assay.

Immunohistochemical staining in human cancer tissue array

Tissue array sides (FDA808k-1, and k-2) were purchased from US Biomax Inc. The list of tissues is given in Table IIa and IIb. Immunohistochemical staining with Remab6-Fab-HRP was performed as described in "Immunohistochemical staining". Isotype human IgG-Fab-HRP was used as a control.

Acknowledgements

We thank Dr. Henrik Clausen for providing Simple Cells, Dr. Tanya McKitrick and Ricky Barnes in the NCFG at BIDMC for help with data collection and analysis and Robert Kardish in the NCFG at BIDMC for printing the glycopeptide/glycan array.

Supplementary data

Supplementary data for this article is available at *Glycobiology* online.

Funding

National Institutes of Health (Grant U01CA168930 to T.J. & R.D.C., P41GM103694 to R.D.C).

Conflict of interest statement

The views expressed in this article are those of the authors and do not necessarily reflect the official policy or position of the US Food and Drug Administration and the Department of Health and Human Services, nor does mention of trade names, commercial products or organizations imply endorsement by the US Government.

Abbreviations

ADC, antibody-drug conjugates; BSM, bovine submaxillary mucin; CDRs, complementarity-determining regions; CFG, Consortium for Functional Glycomics; GBP, glycan-binding protein; HCD, higher-energy collision-induced dissociation; HPA, *Helix pomatia* agglutinin; HRP, horseradish peroxidase; IHC, immunohistochemistry; KO, knockout; mAb, monoclonal antibody; PNA, peanut agglutinin; PTM, posttranslational modification; STn, sialyl-Tn antigen; TACA, tumor-associated carbohydrate antigens; VVA, *Vicia villosa* agglutinin; WT, wild-type

References

Aithal A, Rauth S, Kshirsagar P, Shah A, Lakshmanan I, Junker WM, Jain M, Ponnusamy MP, Batra SK. 2018. MUC16 as a novel target for cancer therapy. *Expert Opin Ther Targets*. 22(8):675–686.

Ando H, Matsushita T, Wakitani M, Sato T, Kodama-Nishida S, Shibata K, Shitara K, Ohta S. 2008. Mouse-human chimeric anti-Tn IgG1 induced anti-tumor activity against Jurkat cells in vitro and in vivo. *Biol Pharm Bull*. 31(9):1739–1744.

Avichezer D, Springer GF, Schechter B, Arnon R. 1997. Immunoreactivities of polyclonal and monoclonal anti-T and anti-Tn antibodies with human carcinoma cells, grown in vitro and in a xenograft model. *Int J Cancer*. 72(1):119–127.

Bennett EP, Mandel U, Clausen H, Gerken TA, Fritz TA, Tabak LA. 2012. Control of mucin-type O-glycosylation: A classification of the polypeptide GalNAc-transferase gene family. *Glycobiology*. 22(6):736–756.

Bern M, Cai Y, Goldberg D. 2007. Lookup peaks: A hybrid of de novo sequencing and database search for protein identification by tandem mass spectrometry. *Anal Chem*. 79(4):1393–1400.

Bigbee WL, Langlois RG, Stanker LH, Vanderlaan M, Jensen RH. 1990. Flow cytometric analysis of erythrocyte populations in Tn syndrome blood using monoclonal antibodies to glycophorin a and the Tn antigen. *Cytometry*. 11(2):261–271.

Blixt O, Lavrova OI, Mazurov DV, Clo E, Kracun SK, Bovin NV, Filatov AV. 2012. Analysis of Tn antigenicity with a panel of new IgM and IgG1 monoclonal antibodies raised against leukemic cells. *Glycobiology*. 22(4):529–542.

Borgert A, Heimburg-Molinaro J, Song X, Lasanajak Y, Ju T, Liu M, Thompson P, Ragupathi G, Barany G, Smith DF et al. 2012. Deciphering structural elements of mucin glycoprotein recognition. *ACS Chem Biol*. 7(6):1031–1039.

Brockhausen I, Yang J, Dickinson N, Ogata S, Itzkowitz SH. 1998. Enzymatic basis for sialyl-Tn expression in human colon cancer cells. *Glycoconj J*. 15(6):595–603.

Brooks CL, Schietinger A, Borisova SN, Kufer P, Okon M, Hirama T, Mackenzie CR, Wang LX, Schreiber H, Evans SV. 2010. Antibody recognition of a unique tumor-specific glycopeptide antigen. *Proc Natl Acad Sci U S A*. 107(22):10056–10061.

Campos D, Freitas D, Gomes J, Magalhaes A, Steentoft C, Gomes C, Vester-Christensen MB, Ferreira JA, Afonso LP, Santos LL et al. 2015. Probing the O-glycoproteome of gastric cancer cell lines for biomarker discovery. *Mol Cell Proteomics*. 14(6):1616–1629.

Chai AW, Cheung AK, Dai W, Ko JM, Ip JC, Chan KW, Kwong DL, Ng WT, Lee AW, Ngan RK et al. 2016. Metastasis-suppressing NID2, an epigenetically-silenced gene, in the pathogenesis of nasopharyngeal carcinoma and esophageal squamous cell carcinoma. *Oncotarget*. 7(48):78859–78871.

Chen ZQ, Huang LS, Zhu B. 2018. Assessment of seven clinical tumor markers in diagnosis of non-small-cell lung cancer. *Dis Markers*. 2018: 9845123.

Chia J, Goh G, Bard F. 2016. Short O-GalNAc glycans: Regulation and role in tumor development and clinical perspectives. *Biochim Biophys Acta*. 1860(8):1623–1639.

Cummings RD. 2009. The repertoire of glycan determinants in the human glycome. *Mol Biosyst*. 5(10):1087–1104.

Danussi C, Coslovi A, Campa C, Mucignat MT, Spessotto P, Uggeri F, Paoletti S, Colombatti A. 2009. A newly generated functional antibody identifies Tn antigen as a novel determinant in the cancer cell-lymphatic endothelium interaction. *Glycobiology*. 19(10):1056–1067.

Fuster MM, Esko JD. 2005. The sweet and sour of cancer: Glycans as novel therapeutic targets. *Nat Rev Cancer*. 5(7):526–542.

Hakomori S. 2001. Tumor-associated carbohydrate antigens defining tumor malignancy: Basis for development of anti-cancer vaccines. *Adv Exp Med Biol*. 491:369–402.

Heimburg-Molinaro J, Song X, Smith DF, Cummings RD. 2011. Preparation and analysis of glycan microarrays. *Curr Protoc Protein Sci*. Chapter 12: Unit12 10.

Hirohashi S, Clausen H, Yamada T, Shimosato Y, Hakomori S. 1985. Blood group a cross-reacting epitope defined by monoclonal antibodies NCC-LU-35 and -81 expressed in cancer of blood group O or B individuals: Its identification as Tn antigen. *Proc Natl Acad Sci U S A*. 82(20):7039–7043.

Ho WL, Chou CH, Jeng YM, Lu MY, Yang YL, Jou ST, Lin DT, Chang HH, Lin KH, Hsu WM et al. 2014. GALNT2 suppresses malignant phenotypes through IGF-1 receptor and predicts favorable prognosis in neuroblastoma. *Oncotarget*. 5(23):12247–12259.

Hofmann BT, Schluter L, Lange P, Mercanoglu B, Ewald F, Folster A, Picksak AS, Harder S, El Gammal AT, Grupp K et al. 2015. COSMC knockdown mediated aberrant O-glycosylation promotes oncogenic properties in pancreatic cancer. *Mol Cancer*. 14:109.

Huang J, Byrd JC, Siddiki B, Yuan M, Lau E, Kim YS. 1992. Monoclonal antibodies against partially deglycosylated colon cancer mucin that recognize Tn antigen. *Dis Markers*. 10(2):81–94.

Hubert P, Heitzmann A, Viel S, Nicolas A, Sastre-Garau X, Oppezzo P, Pritsch O, Osinaga E, Amigorena S. 2011. Antibody-dependent cell cytotoxicity synapses form in mice during tumor-specific antibody immunotherapy. *Cancer Res*. 71(15):5134–5143.

Itzkowitz SH, Bloom EJ, Lau TS, Kim YS. 1992. Mucin associated Tn and sialosyl-Tn antigen expression in colorectal polyps. *Gut*. 33(4): 518–523.

Jiang Y, Liu Z, Xu F, Dong X, Cheng Y, Hu Y, Gao T, Liu J, Yang L, Jia X et al. 2018. Aberrant O-glycosylation contributes to tumorigenesis in human colorectal cancer. *J Cell Mol Med*. 22(10):4875–4885.

Joshi HJ, Jorgensen A, Schjoldager KT, Halim A, Dworkin LA, Steentoft C, Wandall HH, Clausen H, Vakhrushev SY. 2018. GlycoDomainViewer: A bioinformatics tool for contextual exploration of glycoproteomes. *Glycobiology*. 28(3):131–136.

Ju T, Aryal RP, Kudelka MR, Wang Y, Cummings RD. 2014. The Cosmc connection to the Tn antigen in cancer. *Cancer Biomark*. 14(1):63–81.

Ju T, Brewer K, D'Souza A, Cummings RD, Canfield WM. 2002a. Cloning and expression of human core 1 beta1,3-galactosyltransferase. *J Biol Chem*. 277(1):178–186.

Ju T, Cummings RD. 2002b. A unique molecular chaperone Cosmc required for activity of the mammalian core 1 beta 3-galactosyltransferase. *Proc Natl Acad Sci U S A*. 99(26):16613–16618.

Ju T, Lanneau GS, Gautam T, Wang Y, Xia B, Stowell SR, Willard MT, Wang W, Xia JY, Zuna RE et al. 2008. Human tumor antigens Tn and sialyl Tn arise from mutations in Cosmc. *Cancer Res*. 68(6):1636–1646.

Ju T, Wang Y, Aryal RP, Lehoux SD, Ding X, Kudelka MR, Cutler C, Zeng J, Wang J, Sun X et al. 2013. Tn and sialyl-Tn antigens, aberrant O-glycomics as human disease markers. *Proteomics Clin Appl*. 7(9–10):618–631.

Kanoh A, Takeuchi H, Kato K, Waki M, Usami K, Irimura T. 2008. Interleukin-4 induces specific pp-GalNAc-T expression and alterations in mucin O-glycosylation in colonic epithelial cells. *Biochim Biophys Acta*. 1780(3):577–584.

King MJ, Parsons SF, Wu AM, Jones N. 1991. Immunochemical studies on the differential binding properties of two monoclonal antibodies reacting with Tn red cells. *Transfusion*. 31(2):142–149.

Kubota T, Matsushita T, Niwa R, Kumagai I, Nakamura K. 2010. Novel anti-Tn single-chain Fv-Fc fusion proteins derived from immunized phage library and antibody Fc domain. *Anticancer Res*. 30(9):3397–3405.

Kudelka MR, Hinrichs BH, Darby T, Moreno CS, Nishio H, Cutler CE, Wang J, Wu H, Zeng J, Wang Y et al. 2016. Cosmc is an X-linked inflammatory bowel disease risk gene that spatially regulates gut microbiota and contributes to sex-specific risk. *Proc Natl Acad Sci U S A*. 113(51):14787–14792.

Kudelka MR, Ju T, Heimburg-Molinaro J, Cummings RD. 2015. Simple sugars to complex disease–mucin-type O-glycans in cancer. *Adv Cancer Res*. 126:53–135.

Lehoux S, Mi R, Aryal RP, Wang Y, Schjoldager KT, Clausen H, van Die I, Han Y, Chapman AB, Cummings RD et al. 2014. Identification of distinct glycoforms of IgA1 in plasma from patients with immunoglobulin A (IgA) nephropathy and healthy individuals. *Mol Cell Proteomics*. 13(11):3097–3113.

Lin TC, Chen ST, Huang MC, Huang J, Hsu CL, Juan HF, Lin HH, Chen CH. 2017. GALNT6 expression enhances aggressive phenotypes of ovarian cancer cells by regulating EGFR activity. *Oncotarget*. 8(26): 42588–42601.

Longenecker BM, Willans DJ, MacLean GD, Selvaraj S, Suresh MR, Noujaim AA. 1987. Monoclonal antibodies and synthetic tumor-associated glycoconjugates in the study of the expression of Thomsen-Friedenreich-like and Tn-like antigens on human cancers. *J Natl Cancer Inst*. 78(3):489–496.

Matsumoto Y, Zhang Q, Akita K, Nakada H, Hamamura K, Tsuchida A, Okajima T, Furukawa K, Urano T, Furukawa K. 2013. Trimeric Tn antigen on syndecan 1 produced by ppGalNAc-T13 enhances cancer metastasis via a complex formation with integrin alpha5beta1 and matrix metalloproteinase 9. *J Biol Chem*. 288(33):24264–24276.

Mazal D, Lo-Man R, Bay S, Pritsch O, Deriaud E, Ganneau C, Medeiros A, Ubillos L, Obal G, Berois N et al. 2013. Monoclonal antibodies toward different Tn-amino acid backbones display distinct recognition patterns on human cancer cells. Implications for effective immuno-targeting of cancer. *Cancer Immunol Immunother*. 62(6):1107–1122.

Mitchell BS, Schumacher U. 1999. The use of the lectin Helix pomatia agglutinin (HPA) as a prognostic indicator and as a tool in cancer research. *Histol Histopathol*. 14(1):217–226.

Morita N, Yajima Y, Asanuma H, Nakada H, Fujita-Yamaguchi Y. 2009. Inhibition of cancer cell growth by anti-Tn monoclonal antibody MLS128. *Biosci Trends*. 3(1):32–37.

Naito S, Takahashi T, Onoda J, Uemura S, Ohyabu N, Takemoto H, Yamane S, Fujii I, Nishimura SI, Numata Y. 2017. Generation of novel anti-MUC1 monoclonal antibodies with designed carbohydrate specificities using MUC1 glycopeptide library. *ACS Omega*. 2(11): 7493–7505.

Nakamoto Y, Saga T, Sakahara H, Yao Z, Zhang M, Sato N, Zhao S, Nakada H, Yamashina I, Konishi J. 1998. Three-step tumor imaging with biotinylated monoclonal antibody, streptavidin and 111In-DTPA-biotin. *Nucl Med Biol*. 25(2):95–99.

Niang B, Jin L, Chen X, Guo X, Zhang H, Wu Q, Padhiar AA, Xiao M, Fang D, Zhang J. 2016. GalNAc-T4 putatively modulates the estrogen regulatory network through FOXA1 glycosylation in human breast cancer cells. *Mol Cell Biochem*. 411(1–2):393–402.

Numata Y, Nakada H, Fukui S, Kitagawa H, Ozaki K, Inoue M, Kawasaki T, Funakoshi I, Yamashina I. 1990. A monoclonal antibody directed to Tn antigen. *Biochem Biophys Res Commun*. 170(3):981–985.

Osinaga E, Bay S, Tello D, Babino A, Pritsch O, Assemat K, Cantacuzene D, Nakada H, Alzari P. 2000. Analysis of the fine specificity of Tn-binding proteins using synthetic glycopeptide epitopes and a biosensor based on surface plasmon resonance spectroscopy. *FEBS Lett*. 469(1):24–28.

Pancino GF, Osinaga E, Vorauher W, Kakouche A, Mistro D, Charpin C, Roseto A. 1990. Production of a monoclonal antibody as immunohistochemical marker on paraffin embedded tissues using a new immunization method. *Hybridoma*. 9(4):389–395.

Park JH, Katagiri T, Chung S, Kijima K, Nakamura Y. 2011. Polypeptide N-acetylgalactosaminyltransferase 6 disrupts mammary acinar morphogenesis through O-glycosylation of fibronectin. *Neoplasia*. 13(4):320–326.

Park JH, Nishidate T, Kijima K, Ohashi T, Takegawa K, Fujikane T, Hirata K, Nakamura Y, Katagiri T. 2010. Critical roles of mucin 1 glycosyla-

tion by transactivated polypeptide N-acetylgalactosaminyltransferase 6 in mammary carcinogenesis. *Cancer Res*. 70(7):2759–2769.

Persson N, Stuhr-Hansen N, Risinger C, Mereiter S, Polonia A, Polom K, Kovacs A, Roviello F, Reis CA, Welinder C et al. 2017. Epitope mapping of a new anti-Tn antibody detecting gastric cancer cells. *Glycobiology*. 27(7):635–645.

Posey AD Jr, Schwab RD, Boesteanu AC, Steentoft C, Mandel U, Engels B, Stone JD, Madsen TD, Schreiber K, Haines KM et al. 2016. Engineered CAR T cells targeting the cancer-associated Tn-glycoform of the membrane mucin MUC1 control adenocarcinoma. *Immunity*. 44(6):1444–1454.

Radhakrishnan P, Dabelsteen S, Madsen FB, Francavilla C, Kopp KL, Steentoft C, Vakhrushev SY, Olsen JV, Hansen L, Bennett EP et al. 2014. Immature truncated O-glycophenotype of cancer directly induces oncogenic features. *Proc Natl Acad Sci U S A*. 111(39):E4066–E4075.

Reis CA, Sorensen T, Mandel U, David L, Mirgorodskaya E, Roepstorff P, Kihlberg J, Hansen JE, Clausen H. 1998. Development and characterization of an antibody directed to an alpha-N-acetyl-D-galactosamine glycosylated MUC2 peptide. *Glycoconj J*. 15(1):51–62.

Rostami N, Nikkhoo A, Ajjoolabady A, Azizi G, Hojjat-Farsangi M, Ghalamfarsa G, Yousefi B, Yousefi M, Jadidi-Niaragh F. 2019. S1PR1 as a novel promising therapeutic target in cancer therapy. *Mol Diagn Ther*. .

Saeland E, Belo AI, Mongera S, van Die I, Meijer GA, van Kooyk Y. 2012. Differential glycosylation of MUC1 and CEACAM5 between normal mucosa and tumour tissue of colon cancer patients. *Int J Cancer*. 131(1):117–128.

Sakai K, Yuasa N, Tsukamoto K, Takasaki-Matsumoto A, Yajima Y, Sato R, Kawakami H, Mizuno M, Takayanagi A, Shimizu N et al. 2010. Isolation and characterization of antibodies against three consecutive Tn-antigen clusters from a phage library displaying human single-chain variable fragments. *J Biochem*. 147(6):809–817.

Schumacher U, Higgs D, Loizidou M, Pickering R, Leathem A, Taylor I. 1994. Helix pomatia agglutinin binding is a useful prognostic indicator in colorectal carcinoma. *Cancer*. 74(12):3104–3107.

Sedlik C, Heitzmann A, Viel S, Ait Sarkouh R, Batisse C, Schmidt F, De La Rochere P, Amzallag N, Osinaga E, Oppezzo P et al. 2016. Effective antitumor therapy based on a novel antibody-drug conjugate targeting the Tn carbohydrate antigen. *Oncoimmunology*. 5(7):e1171434.

Sheng YH, He Y, Hasnain SZ, Wang R, Tong H, Clarke DT, Lourie R, Oancea I, Wong KY, Lumley JW et al. 2017. MUC13 protects colorectal cancer cells from death by activating the NF-kappaB pathway and is a potential therapeutic target. *Oncogene*. 36(5):700–713.

Singh SK, Streng-Ouwehand I, Litjens M, Kalay H, Saeland E, van Kooyk Y. 2011. Tumour-associated glycan modifications of antigen enhance MGL2 dependent uptake and MHC class I restricted CD8 T cell responses. *Int J Cancer*. 128(6):1371–1383.

Song K, Herzog BH, Fu J, Sheng M, Bergstrom K, McDaniel JM, Kondo Y, McGee S, Cai X, Li P et al. 2015. Loss of core 1-derived O-glycans decreases breast cancer development in mice. *J Biol Chem*. 290(33):20159–20166.

Song KH, Park MS, Nandu TS, Gadad S, Kim SC, Kim MY. 2016. GALNT14 promotes lung-specific breast cancer metastasis by modulating self-renewal and interaction with the lung microenvironment. *Nat Commun*. 7:13796.

Sorensen AL, Reis CA, Tarp MA, Mandel U, Ramachandran K, Sankaranarayanan V, Schwientek T, Graham R, Taylor-Papadimitriou J, Hollingsworth MA et al. 2006. Chemoenzymatically synthesized multimeric Tn/STn MUC1 glycopeptides elicit cancer-specific anti-MUC1 antibody responses and override tolerance. *Glycobiology*. 16(2):96–107.

Springer GF, Chandrasekaran EV, Desai PR, Tegtmeyer H. 1988. Blood group Tn-active macromolecules from human carcinomas and erythrocytes: Characterization of and specific reactivity with mono- and poly-clonal anti-Tn antibodies induced by various immunogens. *Carbohydr Res*. 178:271–292.

Springer GF, Desai PR, Wise W, Carlstedt SC, Tegtmeyer H, Stein R, Scanlon EF. 1990. Pancarcinoma T and Tn epitopes: Autoimmunogens and diagnostic markers that reveal incipient carcinomas and help establish prognosis. *Immunol Ser*. 53:587–612.

Steentoft C, Vakhrushev SY, Joshi HJ, Kong Y, Vester-Christensen MB, Schjoldager KT, Lavrsen K, Dabelsteen S, Pedersen NB, Marcos-Silva L et al. 2013. Precision mapping of the human O-GalNAc glycoproteome through SimpleCell technology. *EMBO J*. 32(10):1478–1488.

Steentoft C, Vakhrushev SY, Vester-Christensen MB, Schjoldager KT, Kong Y, Bennett EP, Mandel U, Wandall H, Levery SB, Clausen H. 2011. Mining the O-glycoproteome using zinc-finger nuclease-glycoengineered SimpleCell lines. *Nat Methods*. 8(11):977–982.

Stowell SR, Ju T, Cummings RD. 2015. Protein glycosylation in cancer. *Annu Rev Pathol*. 10:473–510.

Takahashi HK, Metoki R, Hakomori S. 1988. Immunoglobulin G3 monoclonal antibody directed to Tn antigen (tumor-associated alpha-N-acetylgalactosaminyl epitope) that does not cross-react with blood group A antigen. *Cancer Res*. 48(15):4361–4367.

Tang YA, Chen YF, Bao Y, Mahara S, Yatim S, Oguz G, Lee PL, Feng M, Cai Y, Tan EY et al. 2018. Hypoxic tumor microenvironment activates GLI2 via HIF-1alpha and TGF-beta2 to promote chemoresistance in colorectal cancer. *Proc Natl Acad Sci U S A*. 115(26):E5990–E5999.

Taniuchi K, Cerny RL, Tanouchi A, Kohno K, Kotani N, Honke K, Saibara T, Hollingsworth MA. 2011. Overexpression of GalNAc-transferase GalNAc-T3 promotes pancreatic cancer cell growth. *Oncogene*. 30(49):4843–4854.

Taylor-Papadimitriou J, Burchell JM, Graham R, Beatson R. 2018. Latest developments in MUC1 immunotherapy. *Biochem Soc Trans*. 46(3):659–668.

Thurnher M, Clausen H, Sharon N, Berger EG. 1993. Use of O-glycosylation-defective human lymphoid cell lines and flow cytometry to delineate the specificity of Moluccella laevis lectin and monoclonal antibody 5F4 for the Tn antigen (GalNAc alpha 1-O-Ser/Thr). *Immunol Lett*. 36(3): 239–243.

Tollefsen SE, Kornfeld R. 1983. The B4 lectin from Vicia villosa seeds interacts with N-acetylgalactosamine residues alpha-linked to serine or threonine residues in cell surface glycoproteins. *J Biol Chem*. 258(8):5172–5176.

Tsuji T, T O. 1986. Carbohydrate structures of bovine submaxillary mucin. *Carbohydr Res*. 151:391–402.

Vakhrushev SY, Steentoft C, Vester-Christensen MB, Bennett EP, Clausen H, Levery SB. 2013. Enhanced mass spectrometric mapping of the human GalNAc-type O-glycoproteome with SimpleCells. *Mol Cell Proteomics*. 12(4):932–944.

Vlad AM, Muller S, Cudic M, Paulsen H, Otvos, Jr L, Hanisch FG, Finn OJ. 2002. Complex carbohydrates are not removed during processing of glycoproteins by dendritic cells: Processing of tumor antigen MUC1 glycopeptides for presentation to major histocompatibility complex class II-restricted T cells. *J Exp Med*. 196(11):1435–1446.

Wagner KW, Punnoose EA, Januario T, Lawrence DA, Pitti RM, Lancaster K, Lee D, . von Goetz M, Yee SF, Totpal K et al. 2007. Death-receptor O-glycosylation controls tumor-cell sensitivity to the proapoptotic ligand Apo2L/TRAIL. *Nat Med*. 13(9):1070–1077.

Wang Q, Shen B, Chen L, Zheng P, Feng H, Hao Q, Liu X, Liu L, Xu S, Chen J et al. 2015. Extracellular calumenin suppresses ERK1/2 signaling and cell migration by protecting fibulin-1 from MMP-13-mediated proteolysis. *Oncogene*. 34(8):1006–1018.

Welinder C, Baldetorp B, Borrebaeck C, Fredlund BM, Jansson B. 2011. A new murine IgG1 anti-Tn monoclonal antibody with in vivo anti-tumor activity. *Glycobiology*. 21(8):1097–1107.

White MA, Tsouko E, Lin C, Rajapakshe K, Spencer JM, Wilkenfeld SR, Vakili SS, Pulliam TL, Awad D, Nikolos F et al. 2018. GLUT12 promotes prostate cancer cell growth and is regulated by androgens and CaMKK2 signaling. *Endocr Relat Cancer*. 25(4):453–469.

Wu YM, Liu CH, Hu RH, Huang MJ, Lee JJ, Chen CH, Huang J, Lai HS, Lee PH, Hsu WM et al. 2011. Mucin glycosylating enzyme GALNT2 regulates the malignant character of hepatocellular carcinoma by modifying the EGF receptor. *Cancer Res*. 71(23):7270–7279.

Xu JL, M D. 2000. Diversity in the CDR3 region of V(H) is sufficient for most antibody specificities. *Immunity*. 13(1):37–45.

Yuan M. 1989. The expression of Tn and S-Tn antigens in cancer and premalignant lesion of colorectal tissues by enzyme immunohistochemical method. *Zhonghua Bing Li Xue Za Zhi*. 18(3):211–213.